TIDES

Ernst J.O. Schrama
Delft University of Technology, Faculty of Aerospace Engineering
Kluyverweg 1, 2629 HS Delft, The Netherlands
e-mail: e.j.o.schrama@tudelft.nl

Code: ae4-876

February 7, 2011

Contents

1 Introduction **3**

2 Tide generation **5**
2.1 Introduction . . . 5
2.2 Tide generating potential . . . 5
2.2.1 Proof . . . 5
2.2.2 Work integral . . . 7
2.2.3 Example . . . 9
2.2.4 Some remarks . . . 9
2.3 Darwin symbols and Doodson numbers . . . 9
2.3.1 Tidal harmonic coefficients . . . 10
2.4 Exercises . . . 12

3 Tides deforming the Earth **13**
3.1 Introduction . . . 13
3.2 Solid Earth tides . . . 13
3.3 Long period equilibrium tides in the ocean . . . 14
3.4 Tidal accelerations at satellite altitude . . . 15
3.5 Gravimetric solid earth tides . . . 16
3.6 Reference system issues . . . 17
3.7 Exercises . . . 18

4 Ocean tides **19**
4.1 Introduction . . . 19
4.2 Equations of motion . . . 21
4.2.1 Newton's law on a rotating sphere . . . 21
4.2.2 Assembly step momentum equations . . . 22
4.2.3 Advection . . . 25
4.2.4 Friction . . . 26
4.2.5 Turbulence . . . 26
4.3 Laplace Tidal Equations . . . 27
4.4 Helmholtz equation . . . 29
4.5 Drag laws . . . 30
4.6 Linear and non-linear tides . . . 30
4.7 Dispersion relation . . . 31
4.8 Exercises . . . 33

5 Data analysis methods **34**
5.1 Harmonic Analysis methods . . . 34
5.2 Response method . . . 36
5.3 Exercises . . . 36

6 Load tides **38**
6.1 Introduction . . . 38
6.2 Green functions . . . 38
6.3 Loading of a surface mass layer . . . 38
6.4 Computing the load tide with spherical harmonic functions . . . 39
6.5 Exercises . . . 41

7 Altimetry and tides **42**
7.1 Introduction . . . 42
7.2 Aliasing . . . 42
7.3 Separating ocean tide and load tides . . . 42
7.4 Results . . . 43
7.5 Exercises . . . 43

8 Tidal Energy Dissipation **45**
8.1 Introduction . . . 45
8.2 Tidal energetics . . . 46
8.2.1 A different formulation of the energy equation . . . 48
8.2.2 Integration over a surface . . . 48
8.2.3 Global rate of energy dissipation . . . 49
8.3 Global dissipation rates . . . 51
8.3.1 Models . . . 52
8.3.2 Interpretation . . . 53
8.4 Exercises . . . 53

A Legendre Functions **54**
A.1 Normalization . . . 56
A.2 Some convenient properties of Legendre functions . . . 57
A.2.1 Property 1 . . . 57
A.2.2 Property 2 . . . 58
A.2.3 Property 3 . . . 58
A.3 Convolution integrals on the sphere . . . 58
A.3.1 Proof . . . 59

B Tidal harmonics **60**

Chapter 1

Introduction

The variation in gravitational pull exerted on the Earth by the motion of Sun and Moon and the rotation of the Earth is responsible for long waves in the Earth's ocean which we call "tides". On most places on Earth we experienced tides as a twice daily phenomenon where water levels vary between a couple of decimeters to a few meters. In some bays a funneling effect takes place, and water levels change up to 10 meter. Tides are the longest waves known in oceanography; due to their periodicity they can be predicted well ahead in time. Tides will not only play a role in modeling the periodic rise and fall of sea level caused by lunar and solar forcing. There are also other phenomena that are directly related to the forcing by Sun and Moon.

In chapter 2 we introduce the concept of a tide generating potential whose gradient is responsible for tidal accelerations causing the "solid Earth" and the oceans to deform. In order to get a more complete overview of the topic one must be aware that tidal signals in geophysical measurements are always more complex than the relatively simple formulation of the tide generating potential.

Deformation of the entire Earth due to an elastic response, also referred as solid Earth tides and related issues, is discussed in chapter 3. A good approximation of the solid Earth tide response is obtained by an elastic deformation theory. The consequence of this theory is that solid Earth tides are well described by equilibrium tides multiplied by appropriate scaling constants in the form of Love numbers that are defined by spherical harmonic degree.

Ocean tides show a different behavior than Solid Earth Tides. Hydrodynamic equations that describe the relation between forcing, currents and water levels are discussed in chapter 4. This shows that the response of deep ocean tides is linear, meaning that tidal motions in the deep ocean take place at frequencies that are astronomically determined, but that the amplitudes and phases of the ocean tide follow from a convolution of an admittance function and the tide generating potential. This is not anymore true near the coast where non-linear tides occur at frequencies that are multiples of linear combinations of astronomical tidal frequencies.

Chapter 5 deals with two well known data analysis techniques which are the harmonic analysis method and the response method for determining amplitude and phase at selected tidal frequencies.

Chapter 6 introduces the theory of load tides, which are indirectly caused by ocean tides. Load tides are a significant secondary effect where the lithosphere experiences

motions at tidal frequencies with amplitudes of the order of 5 to 50 mm. Mathematical modelling of load tides is handled by a convolution on the sphere involving Green functions that in turn depend on material properties of the lithosphere, and the distribution of ocean tides that rest on (i.e. load) the lithosphere.

Up to 1990 most global ocean tide models depended on hydrodynamical modelling. The outcome of these models was tuned to obtain solutions that resemble tidal constants observed at a few hunderd points. A revolution was the availability of satellites equipped with radar altimeters that enable estimation of many more tidal constants. This concept is explained in chapter 7 where it is shown that radar observations of the sea drastically improved the accuracy of deep ocean tide models. One of the consequences is that new ocean tide models result in a better understanding of tidal dissipation mechanisms.

Chapter 8 is an optional chapter, it provides background information with regard to the global rate of energy dissipation in the tides. It discusses the consequences on Earth rotation, in literature referred to as tidal braking. Furthermore it explains that the conversion of mechanical tidal energy into other forms of energy can be explained by the difference between a term describing the gravitational work and a second term describing the power flux divergence. The inferred dissipation estimates do provide hints on the nature of the conversion process, for instance, whether the dissipations are related to bottom friction or conversion of barotropic to internal tides which in turn cause mixing of surface waters and the abyssal ocean.

Tidal research involves a wide variety of subjects and not all material is incorporated in these lectures. These notes do for instance not deal with numerical techniques for solving the Laplace tidal equations. In addition I assume a basic knowledge level in the sense that the reader is reasonably familiar with Newton's laws, celestrial mechanics, linear algebra, analysis, Fourier series, and partial differential equations.

Since the first version of these lecuture notes appeared in March 2004 numerous small corrections were included. Appendix A was added to summarize some well known properties of Legendre functions, spherical harmonics and properties of convolution integrals on the sphere. Appendix B explains a method for computing a table of tidal harmonics.

Ernst J.O. Schrama,
Associate Professor Space Geodesy and Geodynamics
Faculty of Aerospace, TU Delft, Netherlands

Chapter 2

Tide generation

2.1 Introduction

It was Newton's Principia (1687) suggesting that the difference between the gravitational attraction of the Moon (and the Sun) on the Earth and the Earth's center are responsible for tides, see also figure 2.1. According to this definition of astronomical tides the corresponding acceleration $\Delta\overline{f}$ becomes:

$$\Delta\overline{f} = \overline{f}_{PM} - \overline{f}_{EM} \tag{2.1}$$

whereby $\overline{f}_{PM}$ and $\overline{f}_{EM}$ are caused by the gravitational attraction of the Moon M. Implementation of eq. (2.1) is as straightforward as computing the lunar ephemeris and evaluating Newton's gravitational law. In practical computations this equation is not applied because it is more convenient to involve a tide generating potential U whose gradient ∇U corresponds to $\Delta\overline{f}$ in eq. (2.1).

2.2 Tide generating potential

To derive U^a we start with a Taylor series of $U = \mu_M/r$ developed at point E in figure 2.1 where μ_M is the Moon's gravitational constant and r the radius of a vector originating at point M. The first-order approximation of this Taylor series is:

$$\Delta\overline{f} = \frac{\mu_M}{r_{EM}^3} \begin{pmatrix} 2 & 0 & 0 \\ 0 & -1 & 0 \\ 0 & 0 & -1 \end{pmatrix} \begin{pmatrix} \Delta x_1 \\ \Delta x_2 \\ \Delta x_3 \end{pmatrix} \tag{2.2}$$

where the vector $(\Delta x_1, \Delta x_2, \Delta x_3)^T$ is originating at point E and whereby x_1 is running from E to M. The proof of equation (2.2) is explained in the following.

2.2.1 Proof

Let

$$U = \frac{\mu}{r}$$

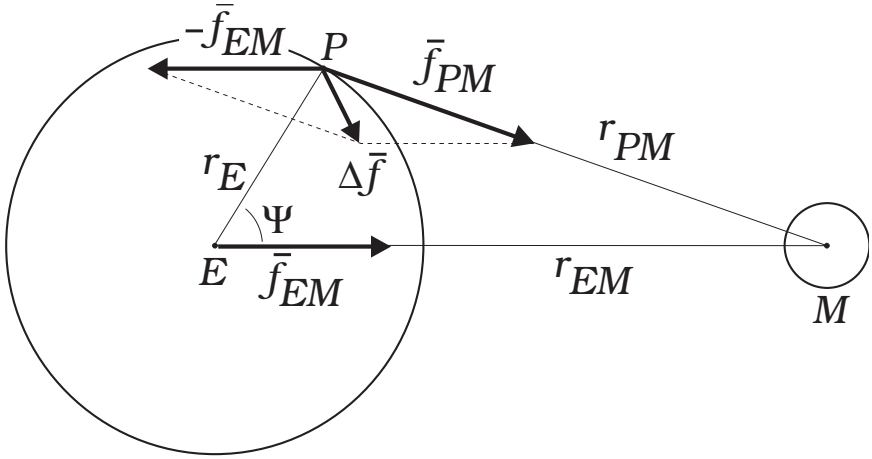

Figure 2.1: The external gravitational force is separated in two components, namely $\overline{f}_{EM}$ and $\overline{f}_{PM}$ whose difference is according to Newton's principia (1687) responsible for the tidal force $\Delta\overline{f}$. Knowledge of the Earth's radius r_E, the Earth-Moon distance r_{EM} and the angle ψ is required to compute a tide generating potential U^a whose gradient ∇U^a corresponds to a tidal acceleration vector $\Delta\overline{f}$.

and

$$r = (x_1^2 + x_2^2 + x_3^2)^{1/2}$$

We find that:

$$\frac{\partial U}{\partial x_i} = -\frac{\mu}{r^3} x_i, \quad i = 1, \cdots, 3$$

and that:

$$\frac{\partial^2 U}{\partial x_i \partial x_j} = 3\frac{\mu}{r^5} x_i x_j - \delta_{ij}\frac{\mu}{r^3}$$

where δ_{ij} is the Kronecker symbol. Here U^a originates from point M and we obtain $\Delta\overline{f}$ by linearizing at:

$$x_1 = r, \quad x_2 = x_3 = 0$$

so that:

$$\left.\frac{\partial^2 U}{\partial x_i \partial x_j}\right|_{\overline{x}=(r,0,0)^T} = \frac{\mu}{r^3}\begin{pmatrix} 2 & 0 & 0 \\ 0 & -1 & 0 \\ 0 & 0 & -1 \end{pmatrix}$$

A first-order approximation of $\Delta\overline{f}$ is $\nabla U|_{(r,0,0)^T}$ at $x_1 = r$, $x_2 = x_3 = 0$:

$$\nabla U|_{(r,0,0)^T} = \left.\frac{\partial^2 U}{\partial x_i \partial x_j}\right|_{(r,0,0)^T} \Delta x_j = \frac{\mu}{r^3}\begin{pmatrix} 2 & 0 & 0 \\ 0 & -1 & 0 \\ 0 & 0 & -1 \end{pmatrix}\begin{pmatrix} \Delta x_1 \\ \Delta x_2 \\ \Delta x_3 \end{pmatrix}$$

where Δx_i for $i = 1, \cdots, 3$ are small displacements at the linearization point E.

2.2.2 Work integral

We continue with equation (2.2) to derive the tide generating potential U^a by evaluation of the work integral:

$$U^a = \int_{s=0}^{r_E} (\Delta\overline{f}, \overline{n})\, ds \tag{2.3}$$

under the assumption that U^a is evaluated on a sphere with radius r_E.

Why a work integral?

A work integral like in eq (2.3) obtains the required amount of Joules to move from A to B through a vector field. An example is "cycling against the wind" which often happens in the Dutch climate. The cyclist goes along a certain path and $\overline{n}$ is the local unit vector in an arbitrary coordinate system. The wind exerts a force $\Delta\overline{f}$, and when each infinitesimal part ds is multiplied by the projection of the wind force on $\overline{n}$ we obtain the required (or provided) work by the wind. For potential problems we deal with a similar situation, except that the force must be replaced by its mass-free equivalent called acceleration and where the acceleration is caused by a gravity effect. In this case the outcome of the work integral yields potential energy difference per mass, which is referred to as potential difference.

Evaluating the work integral

In our case $\overline{n}$ dictates the direction. Keeping in mind the situation depicted in figure 2.1 a logical choice is:

$$\overline{n} = \begin{pmatrix} \cos\psi \\ \sin\psi \\ 0 \end{pmatrix} \tag{2.4}$$

and

$$\begin{pmatrix} \Delta x_1 \\ \Delta x_2 \\ \Delta x_3 \end{pmatrix} = \begin{pmatrix} s\cos\psi \\ s\sin\psi \\ 0 \end{pmatrix} \tag{2.5}$$

so that $(\Delta\overline{f}, \overline{n})$ becomes:

$$\begin{aligned} (\Delta\overline{f}, \overline{n}) &= \frac{\mu_M}{r_{EM}^3} \begin{pmatrix} 2s\cos\psi \\ -s\sin\psi \\ 0 \end{pmatrix} . \begin{pmatrix} \cos\psi \\ \sin\psi \\ 0 \end{pmatrix} \\ &= \frac{s\mu_M}{r_{EM}^3} \left\{ 2\cos^2\psi - \sin^2\psi \right\} \\ &= \frac{s\mu_M}{r_{EM}^3} \left\{ 3\cos^2\psi - 1 \right\} \end{aligned}$$

It follows that:

$$\begin{aligned} U^a &= \int_{s=0}^{r_E} \frac{s\mu_M}{r_{EM}^3} \left\{ 3\cos^2\psi - 1 \right\} .ds \\ &= \frac{\mu_M r_E^2}{r_{EM}^3} \left\{ \frac{3}{2}\cos^2\psi - \frac{1}{2} \right\} \end{aligned} \tag{2.6}$$

$$= \frac{\mu_M r_E^2}{r_{EM}^3} P_2(\cos\psi)$$

which is the first term in the Taylor series where $P_2(\cos\psi)$ is the Legendre function of degree 2. More details on the definition of these special functions are provided in appendix A. But there are more terms, essentially because eq. (2.6) is of first-order. Another example is:

$$\Delta\overline{f_i} = \frac{\partial^3 U}{\partial x_i \partial x_j \partial x_k} \frac{\Delta x_j \Delta x_k}{3!} \tag{2.7}$$

where $U = \mu/r$ for $i, j, k = 1, \cdots, 3$. Without further proof we mention that the second term in the series derived from eq. (2.7) becomes:

$$U^a_{n=3} = \frac{\mu_M r_E^3}{r_{EM}^4} P_3(\cos\psi) \tag{2.8}$$

By induction one can show that:

$$U^a = \frac{\mu_M}{r_{EM}} \sum_{n=2}^{\infty} \left(\frac{r_E}{r_{EM}}\right)^n P_n(\cos\psi) \tag{2.9}$$

represents the full series describing the tide generating potential U^a. In case of the Earth-Moon system $r_E \approx \frac{1}{60} r_{EM}$ so that rapid convergence of eq. (2.9) is ensured. In practice it doesn't make sense to continue the summation in eq. (2.9) beyond $n = 3$.

Equilibrium tides

Theoretically seen eq. (2.9) can be used to compute tidal heights at the surface of the Earth. In a simplified case one could compute the tidal height η as $\eta = g^{-1}U^a$ where g is the acceleration of the Earth's gravity field. Also this statement is nothing more than to evaluate the work integral

$$\int_0^\eta (\overline{f}, \overline{n})\, ds = \int_0^\eta g\, ds = g\eta = U^a$$

assuming that g is constant. Tides predicted in this way are called **equilibrium tides**, they are usually associated with Bernoilli rather than Newton who published the subject in the *Philosophae Naturalis Principea Mathematica*, see also [5]. The equilibrium tide theory assumes that ocean tides propagates with the same speed as celestrial bodies move relative to the Earth. In reality this is not the case, later we will show that the ocean tide propagate at a speed that can be approximated by $\sqrt{g.H}$ where g is the gravitational acceleration and H the local depth of the ocean. It turns out that our oceans are not deep enough to allow diurnal and semi-diurnal tides to remain in equilibrium. Imagine a diurnal wave at the equator, its wavespeed would be equal to $40 \times 10^6/(24 \times 3600) = 463$ m/s. This corresponds to an ocean with a depth of 21.5 km which exceeds an average depth of about 3 to 5 km so that equilibrium tides don't occur.

2.2.3 Example

In the following example we will compute $g^{-1}\,(\mu_M/r_{EM})\,(r_E/r_{EM})^n$, ie. the maximum vertical displacement caused by the tide generating potential caused by Sun and Moon. Reference values used in equation (2.9) are (S:Sun, M:Moon):

$$\begin{array}{llll} \mu_M \approx 4.90 \times 10^{12} & m^3 s^{-2} & r_{EM} \approx 60 \times r_E & \\ \mu_S \approx 1.33 \times 10^{20} & m^3 s^{-2} & r_{ES} \approx 1.5 \times 10^{11} & m \\ r_E \approx 6.40 \times 10^{6} & m & g \approx 9.81 & ms^{-2} \end{array}$$

The results are shown in table 2.1.

	$n=2$	$n=3$
Moon	36.2	0.603
Sun	16.5	0.703×10^{-3}

Table 2.1: Displacements caused by the tide generating potential of Sun and Moon, all values are shown in centimeters.

2.2.4 Some remarks

At the moment we can draw the following conclusions from eq. (2.9):

- The $P_2(\cos\psi)$ term in the equation (2.9) resembles an ellipsoid with its main bulge pointing towards the astronomical body causing the tide. This is the main tidal effect which is, if caused by the Moon, at least 60 times larger than the $n = 3$ term in equation (2.9).
- Sun and Moon are the largest contributors, tidal effects of other bodies in the solar system can be ignored.
- U^a is unrelated to the Earth's gravity field. Also it is unrelated to the acceleration experienced by the Earth revolving around the Sun. Unfortunately there exist many confusing popular science explanations on this subject.
- The result of equation (2.9) is that astronomical tides seem to occur at a rate of 2 highs and 2 lows per day. The reason is of course Earth rotation since the Moon and Sun only move by respectively $\approx 13^\circ$ and $\approx 1^\circ$ per day compared to the 359.02° per day caused by the Earth's spin rate.
- Astronomical tides are too simple to explain what is really going on in nature, more on this issue will be explained other chapters.

2.3 Darwin symbols and Doodson numbers

Since equation (2.9) mainly depends on the astronomical positions of Sun and Moon it is not really suitable for applications where the tidal potential is required. A more

practical approach was developed by Darwin (1883), for references see [5], who invented the harmonic method of tidal analysis and prediction. Darwin's classification scheme assigns "letter-digit combinations", also known as Darwin symbols, to certain main lines in a spectrum of tidal lines. The M_2 symbol is a typical example; it symbolizes the most energetic tide caused by the Moon at a twice daily frequency. Later in 1921, Doodson calculated an extensive table of spectral lines which can be linked to the original Darwin symbols. With the advent of computers in the seventies, Cartwright and Edden (1973), with a reference to Cartwright and Tayler (1971) (hereafter CTE) for certain details, computed new tables to verify the earlier work of Doodson. (More detailed references can be found in [4] and in [5]). The tidal lines in these tables are identified by means of so-called Doodson numbers D which are "computed" in the following way:

$$D = k_1(5 + k_2)(5 + k_3).(5 + k_4)(5 + k_5)(5 + k_6) \tag{2.10}$$

where each $k_1, ..., k_6$ is an array of small integers, corresponding with the description shown in table 2.2, where $5's$ are added to obtain a positive number. For $k_i = 5$ where $i > 0$ one uses an X and for $k_i = 6$ where $i > 0$ one uses an E. In principle there exist infinitely many Doodson numbers although in practice only a few hundred lines remain. To simplify the discussion we divide the table in several parts: a) All tidal lines with equal k_1, which is the same as the order m in spherical harmonics, are said to form *species*. Tidal species indicated with $m = 0, 1, 2$ correspond respectively to long period, daily and twice-daily effects, b) All tidal lines with equal k_1 and k_2 terms are said to form *groups*, c) And finally all lines with equal k_1, k_2 and k_3 terms are said to form *constituents*. In reality it is not necessary to go any further than the constituent level so that a year worth of tide gauge data can be used to define amplitude and phase of a constituent. In order to properly define the amplitude and phase of a constituent we need to define nodal modulation factors which will be explained in chapter 5.

2.3.1 Tidal harmonic coefficients

An example of a table with tidal harmonics is shown in appendix B. Tables B.1 and B.2 contain tidal harmonic coefficients computed under the assumption that accurate planetary ephemeris are available. In reality these planetary ephemeris are provided in the form Chebyshev polynomial coefficients contained in the files provided by for instance the Jet Propulsion Laboratory in Pasadena California USA.

To obtain the tidal harmonics we rely on a method whereby the Doodson numbers are prescribed rather than that they are selected by filtering techniques as in CTE. We recall that the tide generating potential U can be written in the following form:

$$U^a = \frac{\mu_M}{r_{em}} \sum_{n=2,3} \left(\frac{r_e}{r_{em}} \right)^n P_n(\cos\psi) \tag{2.11}$$

The first step in realizing the conversion of equation (2.11) is to apply the addition theorem on the $P_n(\cos\psi)$ functions which results in the following formulation:

$$U^a = \sum_{n=2,3} \sum_{m=0}^{n} \sum_{a=0}^{1} \frac{\mu_m \left(r_e/r_{em}\right)^n}{(2n+1)r_{em}} \overline{Y}_{nma}(\theta_m, \lambda_m) \overline{Y}_{nma}(\theta_p, \lambda_p) \tag{2.12}$$

For details see appendix A. Eq. (2.12) should now be related to the CTE equation for the tide generating potential:

$$U^a = g \sum_{n=2}^{3} \sum_{m=0}^{n} c_{nm}(\lambda_p, t) f_{nm} P_{nm}(\cos\theta_p) \tag{2.13}$$

where $g = \mu/R_e^2$ and for $(n+m)$ even:

$$c_{nm}(\lambda_p, t) = \sum_v H^{(v)} \times [\cos(X_v)\cos(m\lambda_p) - \sin(X_v)\sin(m\lambda_p)] \tag{2.14}$$

while for $(n+m)$ odd:

$$c_{nm}(\lambda_p, t) = \sum_v H^{(v)} \times [\sin(X_v)\cos(m\lambda_p) + \cos(X_v)\sin(m\lambda_p)] \tag{2.15}$$

where it is assumed that:

$$f_{nm} = (2\pi N_{nm})^{-1/2} (-1)^m \tag{2.16}$$

and:

$$N_{nm} = \frac{2}{(2n+1)} \frac{(n+m)!}{(n-m)!} \tag{2.17}$$

whereby it should be remarked that this normalization operator differs from the one used in appendix A. We must also specify the summation over the variable v and the corresponding definition of X_v. In total there are approximately 400 to 500 different terms in the summation of v each consisting of a linear combination of six astronomical elements:

$$X_v = k_1 w_1 + k_2 w_2 + k_3 w_3 + k_4 w_4 - k_5 w_5 + k_6 w_6 \tag{2.18}$$

where $k_1 \ \ldots \ k_6$ are integers and:

$$\begin{array}{rcrcr} w_2 & = & 218.3164 & + & 13.17639648 \text{ T} \\ w_3 & = & 280.4661 & + & 0.98564736 \text{ T} \\ w_4 & = & 83.3535 & + & 0.11140353 \text{ T} \\ w_5 & = & 125.0445 & - & 0.05295377 \text{ T} \\ w_6 & = & 282.9384 & + & 0.00004710 \text{ T} \end{array}$$

where T is provided in Julian days relative to January 1, 2000, 12:00 ephemeris time. (When working in UT this reference modified Julian date equals to 51544.4993.) Finally w_1 is computed as follows:

$$w_1 = 360 * U + w_3 - w_2 - 180.0$$

where U is given in fractions of days relative to midnight. In tidal literature one usually finds the classification of w_1 to w_6 as is shown in table 2.2 where it must be remarked that w_5 is retrograde whereas all other elements are prograde. This explains the minus sign equation (2.18).

Here	Frequency	Cartwright, Doodson	Explanation
k_1,w_1	daily	τ, τ	mean time angle in lunar days
k_2,w_2	monthly	q, s	mean longitude of the moon
k_3,w_3	annual	q', h	mean longitude of the sun
k_4,w_4	8.85 yr	p, p	mean longitude of lunar perigee
k_5,w_5	18.61 yr	N, $-N'$	mean longitude of ascending lunar node
k_6,w_6	20926 yr	p', p_1	mean longitude of the sun at perihelion

Table 2.2: Classification of frequencies in tables of tidal harmonics. The columns contain: [1] the notation used in the Doodson number, [2] the frequency, [3] notation used in tidal literature, [4] explanation of variables.

2.4 Exercises

1. Show that the potential energy difference for 0 to H meter above the ground becomes $m.g.H\ kg.m^2/s^2$. Your answer must start with the potential function $U = -\mu/r$.

2. Show that the outcome of Newton's gravity law for two masses m_1 and m_2 evaluated for one of the masses corresponds to the gradient of a so-called point mass potential function $U = G.m_1/r\ +\ const.$ Verify that the point mass potential function in 3D exactly fullfills the Laplace equation.

3. Show that the function $1/r_{PM}$ in figure 2.1 can be developed in a series of Legendre functions $P_n(\cos\psi)$.

4. Show that a work integral for a closed path becomes zero when the force is equal to a mass times an acceleration for a potential functions that satisfy the Laplace equation.

5. Show that a homogeneous hollow sphere and a solid equivalent generate the same potential field outside the sphere.

6. Compute the ratio between the acceleration terms F_{em} and F_{pm} in figure 2.1 at the Earth's surface. Do this at the Poles and the Lunar sub-point. Example 2.2.3 provides constants that apply to the Earth Moon Sun problem.

7. Assume that the astronomical tide generating potential is developed to degree 2, for which values of ψ is the equilibrium tide zero?

8. Compute the extreme tidal height displacements for the equilibrium tide on Earth caused by Jupiter, its mass ratio with respect to Earth is 317.8.

9. How much observation time is required to separate the S_2 tide from the K_2 tide.

Chapter 3

Tides deforming the Earth

3.1 Introduction

Imagine that the solid Earth itself is somehow deforming under tidal accelerations, i.e. gradients of the tide generating potential. This is not unique to our planet, *all* bodies in the universe experience the same effect. Notorious are moons in the neighborhood of the larger planets such as Saturn where the tidal forces can exceed the maximum allowed stress causing the Moon to collapse.

It must be remarked that the Earth will resist forces caused by the tide generating potential. This was recognized by A.E.H. Love (1927), see [4], who assumed that an applied astronomical tide potential for one tidal line:

$$U^a = \sum_n U_n^a = \sum_n U_n'(r) S_n \exp(j\sigma t) \tag{3.1}$$

where S_n is a surface harmonic, will result in a deformation at the surface of the Earth:

$$\overline{u}_n(R) = g^{-1} \left[h_n(R) S_n \overline{e}_r + l_n(R) \nabla S_n \overline{e}_t \right] U_n'(R) \exp(j\sigma t) \tag{3.2}$$

where $\overline{e}_r$ and $\overline{e}_t$ are radial and tangential unit vectors. The *indirect* potential caused by this solid Earth tide effect will be:

$$\delta U(R) = k_n(R) U_n'(R) S_n \exp(j\sigma t) \tag{3.3}$$

Equations (3.2) and (3.3) contain so-called Love numbers h_n, k_n and l_n describing the "geometric radial", "indirect potential" and "geometric tangential" effects. Finally we remark that Love numbers can be obtained from geophysical Earth models and also from geodetic space technique such as VLBI, see table 3.1 taken from [16], where we present the Love numbers reserved for the deformations by a volume force, or potential, that does not load the surface. Loading is described by separate Love numbers h_n', k_n' and l_n' that will be discussed in chapter 6.

3.2 Solid Earth tides

According to equations (3.2) and (3.3) the solid Earth itself will deform under the tidal forces. Well observable is the vertical effect resulting in height variations at geodetic

	Dziewonski-Anderson			Gutenberg-Bullen		
n	h_n	k_n	l_n	h_n	k_n	l_n
2	0.612	0.303	0.0855	0.611	0.304	0.0832
3	0.293	0.0937	0.0152	0.289	0.0942	0.0145
4	0.179	0.0423	0.0106	0.175	0.0429	0.0103

Table 3.1: Love numbers derived from the Dziewonski-Anderson and the Gutenberg-Bullen Earth models.

length	NS baselines	EW baselines
1°	0.003	0.004
2°	0.006	0.009
5°	0.016	0.022
10°	0.031	0.043
20°	0.063	0.084
50°	0.145	0.186
90°	0.134	0.237

Table 3.2: The maximum solid earth tide effect [m] on the relative vertical coordinates of geodetic stations for North-South and East-West baselines varying in length between 0 and 90° angular distance.

stations. To compute the so-called solid-Earth tide η_s we represent the tide generating potential as the series:

$$U^a = \sum_{n=2}^{\infty} U_n^a$$

so that:

$$\eta_s = g^{-1} \sum_{n=2}^{\infty} h_n U_n^a \tag{3.4}$$

An example of η_s is shown in table 3.2 where the extreme values of $|\eta_s|$ are tabulated as a relative height of two geodetic stations separated by a certain spherical distance. One may conclude that regional GPS networks up to e.g. 200 by 200 kilometers are not significantly affected by solid earth tides; larger networks are affected and a correction must be made for the solid Earth tide. The correction itself is probably accurate to within 1 percent or better so that one doesn't need to worry about errors in excess of a couple of millimeters.

3.3 Long period equilibrium tides in the ocean

At periods substantially longer than 1 day the oceans are in equilibrium with respect to the tide generating potential. But also here the situation is more complicated than one

immediately expects from equation (2.9) due to the existence of k_n in equation (3.3). For this reason long period equilibrium tides in the oceans are derived by:

$$\eta_e = g^{-1} \sum_n (1 + k_n - h_n) U_n^a \tag{3.5}$$

essentially because the term $(1 + k_n)$ dictates the geometrical shape of the oceans due to the tide generating potential but also the indirect or induced potential $k_n U_n^a$. Still there is a need to include $-h_n U_n^a$ since ocean tides are always relative to the sea floor or land which is already experiencing the solid earth tide effect η_s described in equation (3.4). Again we emphasize that equation (3.5) is only representative for a long periodic response of the ocean tide which is in a state of equilibrium. Hence equation (3.5) must only be applied to all $m = 0$ terms in the tide generating potential.

3.4 Tidal accelerations at satellite altitude

The astronomical tide generating potential U at the surface of the Earth with radius r_e has the usual form:

$$U(r_e) = \frac{\mu_p}{r_p} \sum_{n=2}^{\infty} (r_e/r_p)^n \, P_n(\cos\psi) = \frac{\mu_p}{r_e} \sum_{n=2}^{\infty} (r_e/r_p)^{n+1} \, P_n(\cos\psi) \tag{3.6}$$

The potential can also be used directly at the altitude of the satellite to compute gradients, but in fact there is no need to do this since the accelerations can be derived from Newton's definition of tidal forces. This procedure does not anymore work for the induced or secondary potential $U'(r_e)$ since the theory of Love predicts that:

$$U'(r_e) = \frac{\mu_p}{r_e} \sum_{n=2}^{\infty} (r_e/r_p)^{n+1} \, k_n P_n(\cos\psi) \tag{3.7}$$

where it should be remarked that this expression is the result of a deformation of the Earth as a result of tidal forcing. The effect at satellite altitude should be that of an upward continuation, in fact, it is a mistake to replace r_e by the satellite radius r_s in the last equation. Instead to bring $U'(r_e)$ to $U'(r_s)$ we get the expression:

$$U'(r_s) = \frac{\mu_p}{r_e} \sum_{n=2}^{\infty} (r_e/r_s)^{n+1} \, (r_e/r_p)^{n+1} \, k_n P_n(\cos\psi) \tag{3.8}$$

Finally we eliminate $\cos(\psi)$ by use of the addition theorem of Legendre functions:

$$U'(r_s) = \frac{\mu_p}{r_e} \sum_{n=2}^{\infty} \left(\frac{r_e^2}{r_s r_p} \right)^{n+1} \frac{k_n}{2n+1} \sum_{m=0}^{n} \overline{P}_{nm}(\cos\theta_p) \overline{P}_{nm}(\cos\theta_s) \cos(m(\lambda_s - \lambda_p)) \tag{3.9}$$

where $(r_s, \theta_s, \lambda_s)$ and $(r_p, \theta_p, \lambda_p)$ are spherical coordinates in the terrestial frame respectively for the satellite and the planet in question. This is the usual expression as it can be found in literature, see for instance [16].

Gradients required for the precision orbit determination (POD) software packages are derived from $U(r_s)$ and $U'(r_s)$ first in spherical terrestial coordinates which are then

transformed via the appropriate Jacobians into terrestial Cartesian coordinates and later in inertial Cartesian coordinates which appear in the equations of motion in POD. Differentiation rules show that the latter transformation sequence follows the transposed transformation sequence compared to that of vectors.

Satellite orbit determination techniques allow one to obtain in an indepent way the k_2 Love number of the Earth or of an arbitrary body in the solar system. Later in these notes it will be shown that similar techniques also allow to estimate the global rate of dissipation of tidal energy, essentially because tidal energy dissipation result in a phase lag between the tidal bulge and the line connecting the Earth to the external planet for which the indirect tide effect is computed.

3.5 Gravimetric solid earth tides

A gravimeter is an instrument for observing the actual value of gravity. There are several types of instruments, one type measures gravity difference between two locations, another type measures the absolute value of gravity. The measured quantity is usually expressed in milligals (mgals) relative to an Earth reference gravity model. The milligal is not a S.I. preferred unit, but it is still used in research dealing with gravity values on the Earth's surface, one mgal equals $10^{-5}\ m/s^2$, and the static variations referring to a value at the mean sea level vary between -300 to +300 mgal. Responsible for these static variations are density anomalies inside the Earth.

Gravimeters do also observe tides, the range is approximately 0.1 of a mgal which is within the accuracy of modern instruments. Observed are the direct astronomical tide, the indirect solid earth tide but also the height variations caused by the solid Earth tides. According to [18] we have the following situation:

$$V = V_0 + \eta_s \frac{\partial V_0}{\partial r} + U^a + U^I \tag{3.10}$$

where V is the observed potential, V_0 is the result of the Earth's gravity field, η_s the vertical displacement implied by the solid Earth tide, U^a is the tide generating potential and U^i the indirect solid Earth tide potential. In the following we assume that:

$$U^a = \sum_n \left(\frac{r}{r_0}\right)^n U_n^a$$

$$U^i = \sum_n \left(\frac{r_0}{r}\right)^{n+1} k_n U_n^a$$

$$\frac{\partial V}{\partial r} = \frac{\mu}{r^2} = -g$$

where μ is the Earth's gravitational constant, r_0 the mean equatorial radius, and U_n^a the tide generating potential at r_0. Note that in the definition of the latter equation we have taken the potential as a negative function on the Earth surface where μ attains a positive value. This is also the correct convention since the potential energy of a particle must be increased to lift it from the Earth surface and it must become zero at infinity. We get:

$$\frac{\partial V}{\partial r} = \frac{\partial V_0}{\partial r} + \eta_s \frac{\partial^2 V}{\partial r^2} + \frac{\partial U^a}{\partial r} + \frac{\partial U^i}{\partial r}$$

which becomes:

$$\frac{\partial V}{\partial r} = \frac{\partial V_0}{\partial r} + \frac{2g}{r}\eta_s + \sum_n \left(\frac{n}{r}\right)\left(\frac{r}{r_0}\right)^n U_n^a - \sum_n \frac{(n+1)}{r}\left(\frac{r_0}{r}\right)^{n+1} k_n U_n^a$$

where $\partial^2 V/\partial r^2$ is approximated by $2g/r$ assuming a point mass potential function. When substituting the solid Earth tide effect η_s we get:

$$\frac{\partial V}{\partial r} = \frac{\partial V_0}{\partial r} + \frac{2g}{r}\sum_n h_n U_n^a g^{-1} + \sum_n \left(\frac{n}{r}\right)\left(\frac{r}{r_0}\right)^n U_n^a - \sum_n \frac{(n+1)}{r}\left(\frac{r_0}{r}\right)^{n+1} k_n U_n^a$$

so that for $r \approx r_0$:

$$\frac{\partial V}{\partial r} = \frac{\partial V_0}{\partial r} + \sum_n \left\{\frac{2h_n}{n} + 1 - \left(\frac{n+1}{n}\right)k_n\right\}\frac{nU_n^a}{r}$$

which becomes:

$$-g = -g_0 + \sum_n \left\{1 + \frac{2}{n}h_n - \left(\frac{n+1}{n}\right)k_n\right\}\frac{\partial U_n^a}{\partial r}$$

On gravity anomalies the effect becomes:

$$\Delta g = g - g_0 = -\sum_n \left\{1 + \frac{2}{n}h_n - \left(\frac{n+1}{n}\right)k_n\right\}\frac{\partial U_n^a}{\partial r}$$

The main contribution comes from the term:

$$\Delta g = -\left\{1 + h_2 - \frac{3}{2}k_2\right\}\frac{\partial U_2^a}{\partial r} = -1.17\frac{\partial U_2^a}{\partial r}$$

while a secondary contribution comes from the term:

$$\Delta g = -\left\{1 + \frac{2}{3}h_3 - \frac{4}{3}k_3\right\}\frac{\partial U_3^a}{\partial r} = -1.07\frac{\partial U_3^a}{\partial r}$$

This shows that gravimeters in principle sense a scaled version of the astronomic tide potential, the factors 1.17 and 1.07 are called gravimetric factors. By doing so gravimetric observations add their own constraint to the definition of the Love numbers h_2 and k_2 and also h_3 and k_3.

3.6 Reference system issues

In view of equation (3.5) we must be careful in defining parameters modeling the reference ellipsoid. The reason is due to a contribution of the tide generating potential at Doodson number 055.555 where it turns out that:

$$g^{-1}U_2^a = -0.19844 \times P_{2,0}(\sin\phi) \quad (3.11)$$

$$g^{-1}k_2 U_2^a = -0.06013 \times P_{2,0}(\sin\phi) \quad (3.12)$$

$$g^{-1}(1+k_2)U_2^a = -0.25857 \times P_{2,0}(\sin\phi) \quad (3.13)$$

where we have assumed that $k_2 = 0.303$, $h_2 = 0.612$ and $H^{(v)} = -0.31459$ at Doodson number 055.555. The question "which equation goes where" is not as trivial as one might think. In principle there are three tidal systems, and the definition is as follows:

- A tide free system: this means that eqn. (3.13) is removed from the reference ellipsoid flattening.
- A zero-tide system: this means that eqn. (3.11) is removed but that (3.12) is not removed from the reference ellipsoid flattening.
- A mean-tide system: this means that eqns. (3.13) is not removed from the reference ellipsoid.

Important in the discussion is that the user of a reference system must be aware which choice has been made in the definition of the flattening parameter of the reference ellipsoid. The International Association of Geodesy recommends a zero-tide system so that it is not necessary to define k_2 at the zero frequency. In fact, from a rheologic perspective it is unclear which value should be assigned to k_2, the IAG recommendation is therefore the most logical choice.

3.7 Exercises

1. Show that the Love numbers h_2 and k_2 can be estimated from observations of the gravimeter tide in combination with observations of the long periodic ocean tide observed by tide gauges.
2. What are the extreme variations in the water level of the M_2 equilibrium tide at a latitude of 10N.
3. What are the extreme variations in mgal of the M_2 gravimetric tide at a latitude of 50S.
4. What is the largest relative gravimetric tidal effect between Amsterdam and Paris as a result of the Moon.
5. Verify equation (3.11), how big is this effect between Groningen and Brussel.

Chapter 4

Ocean tides

4.1 Introduction

Purpose of this chapter is to introduce some basic properties concerning the dynamics of fluids that is applicable to the ocean tide problem. Of course the oceans themselves will respond differently to the tide generating forces. Ocean tides are exactly the effect that one observes at the coast; i.e. the long periodic, diurnal and semi-diurnal motions between the sea surface and the land. In most regions on Earth the ocean tide effect is approximately 0.5 to 1 meters whereas in some bays found along the coast of e.g. Normandy and Brittany the tidal wave is amplified to 10 meters. Ocean tides may have great consequences for daily life and also marine biology in coastal areas. Some islands such as Mt. Saint Michèle in Brittany can't be reached during high tide if no separate access road would exist. A map of the global M_2 ocean tide is given in figure 4.1 from which one can see that there are regions without any tide which are called amphidromes where a tidal wave is continuously rotating about a fixed geographical location. If we ignore friction then the orientation of the rotation is determined by the balance between the pressure gradient and the Coriolis force. It was Laplace who laid the foundations for modern tidal research, his main contributions were:

- The separation of tides into distinct *Species* of long period, daily and twice daily (and higher) frequencies.
- The (almost exact) dynamic equations linking the horizontal and vertical displacement of water particles with the horizontal components of the tide-raising force.
- The hypothesis that, owing to the dominant linearity of these equations, the tide at any place will have the same spectral frequencies as those present in the generating force.

Laplace derived solutions for the dynamic equations only for the ocean and atmospheres covering a globe, but found them to be *strongly dependent on the assumed depth of fluid*. Realistic bathymetry and continental boundaries rendered Laplace's solution mathematically intractable. To explain this problem we will deal with the following topics:

- Define the equations of motion

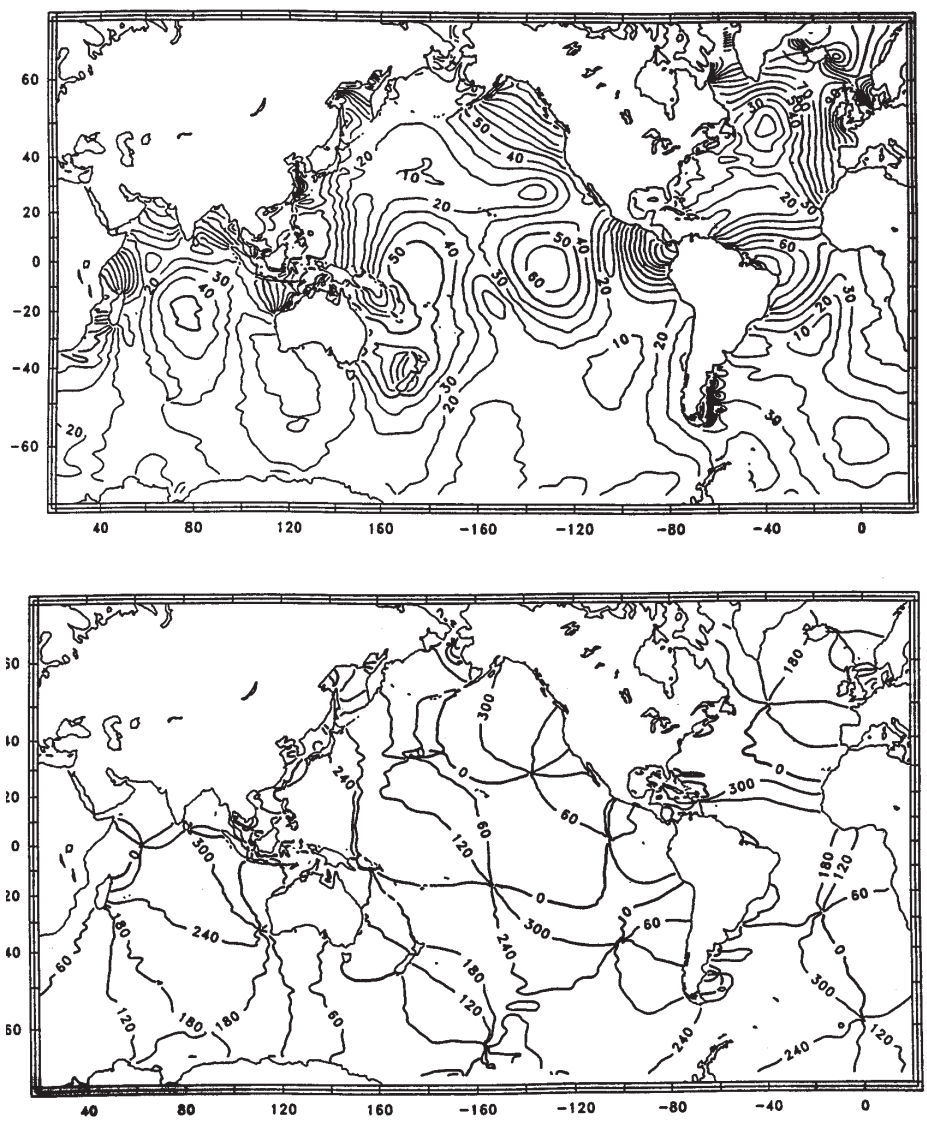

Figure 4.1: The top panel shows the amplitudes in centimeter of the M_2 ocean tide, the bottom panel shows the corresponding phase map.

- What is advection, friction and turbulence
- The Navier Stokes equations
- Laplace tidal equations
- A general wave solution, the Helmholtz equation
- Dispersion relations

However we will avoid to represent a complete course in physical oceanography; within the scope of this course on tides we have to constrain ourselves to a number of essential assumptions and definitions.

4.2 Equations of motion

4.2.1 Newton's law on a rotating sphere

The oceans can be seen as a thin rotating shell with a thickness of approximately 5 km relative on a sphere with an average radius of 6371 km. To understand the dynamics of fluids in this thin rotating shell we initially consider Newton's law $f = m.a$ for a given water parcel at a position:

$$\overline{x} = \overline{e}_i x^i = \overline{e}_a x^a \tag{4.1}$$

In this equation $\overline{e}_i$ and $\overline{e}_a$ are base vectors. Here the i index is used for the inertial coordinate frame, the local Earth-fixed coordinate system gets index a. Purpose of the following two sections will be to find expressions for inertial velocities and accelerations and their expressions in the Earth fixed system, which will appear in the equations of motion in fluid dynamics.

Inertial velocities and accelerations

There is a unique relation between the inertial and the Earth-fixed system given by the transformation:

$$\overline{e}_i = R_i^a \overline{e}_a \tag{4.2}$$

In the inertial coordinate system, velocities can be derived by a straightforward differentiation so that:

$$\dot{\overline{x}} = \overline{e}_i \dot{x}^i \tag{4.3}$$

and accelerations are obtained by a second differentiation:

$$\ddot{\overline{x}} = \overline{e}_i \ddot{x}^i \tag{4.4}$$

Note that this approach is only possible in an inertial frame, which is a frame that does not rotate or accelerate by itself. If the frame would accelerate or rotate then $\overline{e}_i$ also contains derivatives with respect to time. This aspect is worked out in the following section.

Local Earth fixed velocities and accelerations

The Earth fixed system is not an inertial system due to Earth rotation. In this case the base vectors themselves follow different differentiation rules:

$$\dot{\overline{e}}_a = \overline{\omega} \times \overline{e}_a \tag{4.5}$$

where $\overline{\omega}$ denotes the vector $(0, 0, \Omega)$ for an Earth that is rotating about its z-axis at a constant speed of Ω radians per second. We find:

$$\ddot{\overline{e}}_a = \dot{\overline{\omega}} \times \overline{e}_a \ + \ \overline{\omega} \times \overline{\omega} \times \overline{e}_a \tag{4.6}$$

and:

$$\ddot{\overline{x}} = \ddot{\overline{e}}_a x^a \ + \ 2\dot{\overline{e}}_a \dot{x}^a \ + \ \overline{e}_a \ddot{x}^a \tag{4.7}$$

which is equivalent to:

$$\ddot{\overline{x}} = \dot{\overline{\omega}} \times \overline{e}_a x^a \ + \ \overline{\omega} \times \overline{\omega} \times \overline{e}_a x^a \ + \ 2\,\overline{\omega} \times \overline{e}_a \dot{x}^a \ + \ \overline{e}_a \ddot{x}^a \tag{4.8}$$

leading to the equation:

$$\ddot{\overline{x}}_i = \ddot{\overline{x}}_a \ + \ 2\,\overline{\omega} \times \dot{\overline{x}}_a \ + \ \dot{\overline{\omega}} \times \overline{x}_a \ + \ \overline{\omega} \times \overline{\omega} \times \overline{x}_a \tag{4.9}$$

where $\ddot{\overline{x}}_i$ is the inertial acceleration vector, $\ddot{\overline{x}}_a$ the Earth-fixed acceleration vector. The difference between these vectors is the result of frame accelerations:

- The term $2\,\overline{\omega} \times \dot{\overline{x}}_a$ is known as the Coriolis effect. Consequence of the Coriolis effect is that particles moving over the surface of the Earth will experience an apparent force directed perpendicular to their direction. On Earth the Coriolis force is directed to East when a particle is moving to the North on the Northern hemisphere.
- The term $\overline{\omega} \times \overline{\omega} \times \overline{x}_a$ is a centrifugal contribution. This results in an acceleration component that is directed away from the Earth's spin axis.
- The term $\dot{\overline{\omega}} \times \overline{x}_a$ indicates a rotational acceleration which can be ignored unless one intends to consider the small variations in the Earth's spin vector $\overline{\omega}$.

4.2.2 Assembly step momentum equations

To obtain the equations of motion for fluid problems we will consider all relevant accelerations that act on a water parcel in the Earth's fixed frame:

- $\overline{g}$ is the sum of gravitational and centrifugal accelerations, ie. the gravity acceleration vector,
- $-2\overline{\omega} \times \overline{u}$ is the Coriolis effect which is an apparent acceleration term caused by Earth rotation,
- $\overline{f}$ symbolizes additional accelerations which are for instance caused by friction and advection in fluids,
- $-\rho^{-1}\nabla p$ is the pressure gradient in a fluid.

The latter two terms are characteristic for motions of fluids and gasses on the Earth's surface. The pressure gradient is the largest, and it will be explained first because it appears in all hydrodynamic models.

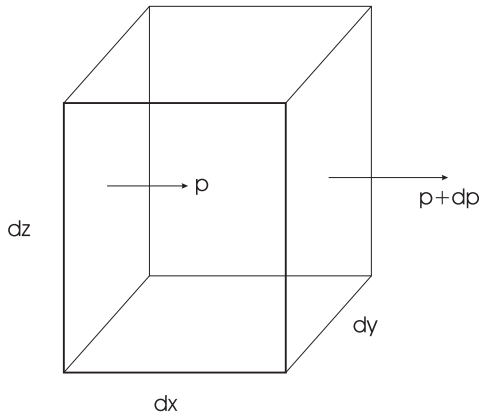

Figure 4.2: Pressure gradient

The pressure gradient

This gradient follows from the consideration of a pressure change on a parcel of water as shown in figure 4.2. In this figure there is a pressure p acting on the western face $dy.dz$ and a pressure $p + dp$ acting on the eastern face $dy.dz$. To obtain a force we multiply the pressure term times the area on which it is acting. The difference between the forces is only relevant since p itself could be the result of a static situation:

$$p.dy.dz - (p + dp)dy.dz = -dpdydz$$

To obtain a force by volume one should divide this expression by $dx.dy.dz$ to obtain:

$$-\frac{\partial p}{\partial x}$$

To obtain a force by mass one should divide by $\rho.dx.dy.dz$ to obtain:

$$-\frac{1}{\rho}\frac{\partial p}{\partial x}$$

This expression is the acceleration of a parcel towards the East which is our x direction. To obtain the acceleration vector of the water parcel one should compute the gradient of the pressure field p and scale with the term $-1/\rho$.

Geostrophic balance

The following expression considers the balance between local acceleration, the pressure gradient, the Coriolis effect and residual forces $\overline{f}$:

$$\frac{D\,\overline{u}}{D\,t} = -\frac{1}{\rho}\nabla p \;-\; 2\,\overline{\omega} \times \overline{u} \;+\; \overline{g} \;+\; \overline{f}. \tag{4.10}$$

This vector equation could also be formulated as three separate equations with the local coordinates x, y and z and the corresponding velocity components u, v and w. Here we

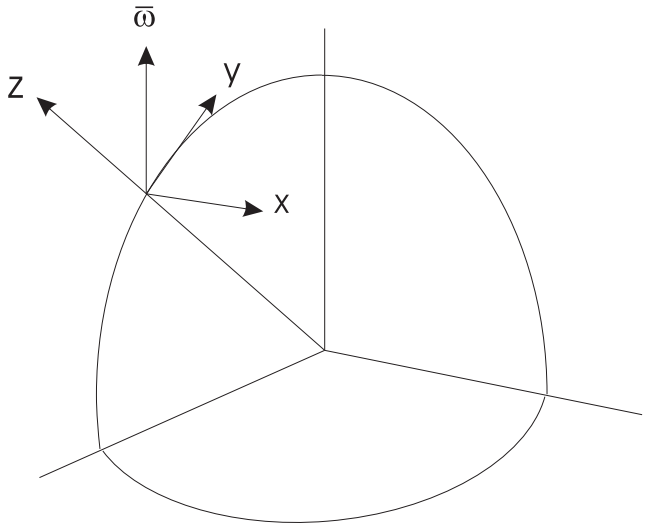

Figure 4.3: Choice of the local coordinate system relevant to the equations of motion.

follow the convention found in literature and assign the x-axis direction corresponding with the u-velocity component to the local east, the y-axis direction and corresponding v-velocity component to the local north, and the z-axis including the w-velocity pointing out of the sea surface, see also figure 4.3. All vectors in equation (4.10) must be expressed in the local x, y, z coordinate frame. If ϕ corresponds to the latitude of the water parcel and Ω to the length of $\overline{\omega}$ then the following substitutions are allowed:

$$\begin{aligned} \overline{\omega} &= (0, \Omega\cos\phi, \Omega\sin\phi)^T \\ \overline{g} &= (0, 0, -g)^T \\ \overline{f} &= (F_x, F_y, F_z)^T \\ \overline{v} &= (u, v, w)^T \end{aligned}$$

The result after substitution is the equations of motions in three dimensions:

$$\begin{aligned} \frac{D\,u}{D\,t} &= -\frac{1}{\rho}\frac{\partial p}{\partial x} + F_x + 2\Omega\sin\phi\, v - 2\Omega\cos\phi\, w \\ \frac{D\,v}{D\,t} &= -\frac{1}{\rho}\frac{\partial p}{\partial y} + F_y - 2\Omega\sin\phi\, u \\ \frac{D\,w}{D\,t} &= -\frac{1}{\rho}\frac{\partial p}{\partial z} + F_z + 2\Omega\cos\phi\, u - g \end{aligned} \tag{4.11}$$

Providing that we forget about dissipative and advective terms eqns. (4.11) tell us nothing more than that the pressure gradient, the Coriolis force and the gravity vector are in balance, see also figure 4.4. Some remarks with regard to the importance of acceleration terms in eqns. (4.11)(a-c):

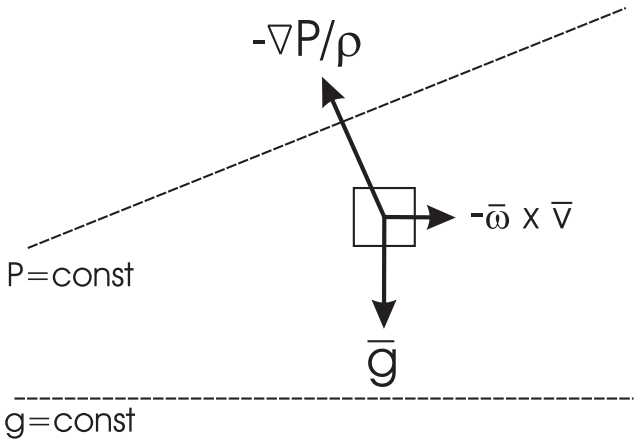

Figure 4.4: The equations of motion is dynamical oceanography, the Coriolis force, the pressure gradient and the gravity vector are in balance.

- The vertical velocity w is small and we will drop this term.
- In eq. (4.11)(c) the gravity term and the pressure gradient term dominate, cancellation of the other terms results in the hydrostatic equation telling us that pressure linearly increases by depth.
- The term $f = 2\Omega \sin \phi$ is called the Coriolis parameter.

4.2.3 Advection

The terms Du/Dt, Dv/Dt and Dw/Dt in eqns. (4.11) should be seen as absolute derivatives. In reality these expressions contain an advective contribution.

$$\begin{aligned}
\frac{D\,u}{D\,t} &= \frac{\partial u}{\partial t} + u.\frac{\partial u}{\partial x} + v.\frac{\partial u}{\partial y} + w.\frac{\partial u}{\partial z} \\
\frac{D\,v}{D\,t} &= \frac{\partial v}{\partial t} + u.\frac{\partial v}{\partial x} + v.\frac{\partial v}{\partial y} + w.\frac{\partial v}{\partial z} \\
\frac{D\,w}{D\,t} &= \frac{\partial w}{\partial t} + u.\frac{\partial w}{\partial x} + v.\frac{\partial w}{\partial y} + w.\frac{\partial w}{\partial z}
\end{aligned} \tag{4.12}$$

In literature terms like $\partial u/\partial t$ are normally considered as so-called "local accelerations" whereas advective terms like $u\partial u/\partial x + ...$ are considered as "field accelerations". The physical interpretation is that two types of acceleration may take place. In the first terms on the right hand side, accelerations occur locally at the coordinates (x, y, z) resulting in $\partial u/\partial t$, $\partial v/\partial t$, and $\partial w/\partial t$ whereas in the second case the velocity vector is changing

with respect to the coordinates resulting in advection. This effect is non-linear because velocities are squared, (e.g. $u(\partial u/\partial x) = \frac{1}{2}[\partial(u^2)/\partial x]$).

4.2.4 Friction

In eq. (4.11) friction may appear in F_x, F_y and F_z. Based upon observational evidence, Stokes suggested that tangentional stresses are related to the velocity shear as:

$$\tau_{ij} = \mu \ (\partial u_i/\partial x_j + \partial u_j/\partial x_i) \tag{4.13}$$

where μ is a molecular viscosity coefficient characteristic for a particular fluid. Frictional forces are obtained by:

$$F = \frac{\partial \tau_{ij}}{\partial x_j} = \mu \frac{\partial^2 u_i}{\partial {x_j}^2} + \mu \frac{\partial}{\partial x_i}\left(\frac{\partial u_i}{\partial x_j}\right) \tag{4.14}$$

which is approximated by:

$$F = \mu \frac{\partial^2 u_i}{\partial {x_j}^2} \tag{4.15}$$

if an incompressible fluid is assumed. A separate issue is that viscosity $\nu = \mu/\rho$ may not be constant because of turbulence. In this case:

$$F = \frac{\partial \tau_{ij}}{\partial x_j} = \frac{\partial}{\partial x_j}\left(\mu \frac{\partial u_i}{\partial x_j}\right) \tag{4.16}$$

although it should be remarked that also this equation is based upon an assumption. As a general rule, no known oceanic motion is controlled by molecular viscosity, since it is far too weak. In ocean dynamics the "Reynold stress" involving turbulence or eddy viscosity always applies, see also [19] or [25].

4.2.5 Turbulence

Fluid motions often show a turbulent behavior whereby energy contained in small scale phenomena transfer their energy to larger scales. In order to assess whether turbulence occurs in an experiment we define the so-called Reynolds number Re which is a measure for the ratio between advective and the frictional terms. The Reynolds number is approximated as $Re = U.L/\nu$, where U and L are velocities and lengths at the characteristic scales at which the motions occurs. Large Reynolds numbers, e.g. ones which are greater than 1000, usually indicates turbulent flow.

An example of this phenomenon can be found in the Gulf stream area where L is of the order of 100 km, U is of the order of 1 m/s and a typical value for ν is approximately 10^{-6} $m^2 s^{-1}$ so that $Re = U.L/\nu \approx 10^{11}$. The effect displays itself as a meandering of the main stream which can be nicely demonstrated by infrared images of the area showing the turbulent flow of the Gulf stream occasionally releasing eddies that will live for considerable time in the open oceans. The same phenomenon can be observed in other western boundary regions of the oceans such as the Kuroshio current East of Japan and the Argulhas retroreflection current south of Cape of Good Hope.

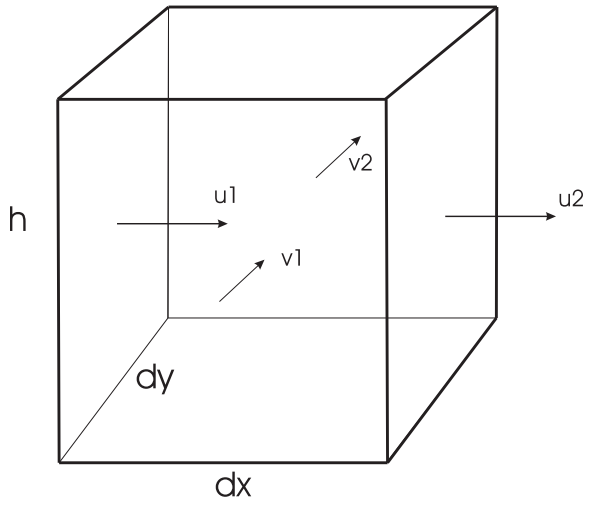

Figure 4.5: Continuity and depth averaged velocities

4.3 Laplace Tidal Equations

So far the equations of motions are formulated in three dimensions. The goal of the Laplace Tidal Equations is in first instance to simplify this situation. Essentially the LTE describe the motions of a *depth averaged velocity* fluid dynamics problem. Rather than considering the equations of motion for a parcel of water in three dimensions, the problem is scaled down to two dimensions in x and y whereby the former is locally directed to the east and the latter locally directed to the north. A new element in the discussion is a consideration of the continuity equation.

To obtain the LTE we consider a box of water with the ground plane dimensions dx times dy and height h representing the mean depth of the ocean, see also figure 4.5. Moreover let u_1 be the mean columnar velocity of water entering the box via the $dy \times h$ plane from the west and u_2 the mean velocity of water leaving the box via the $dy \times h$ plane to the east. Also let v_1 be the mean columnar velocity of water entering the box via the $dx \times h$ plane from the south and v_2 the mean velocity of water leaving the $dx \times h$ plane to the north. In case there are no additional sources or drains (like a hole in the ocean floor or some river adding water to it) we find that:

$$h.dy.(u_2 - u_1) + h.dx.(v_2 - v_1) + \frac{dV}{dt} = 0 \tag{4.17}$$

where the volume V is computed as $dx.dy.h$. Take η as the surface elevation due to the in-flux of water and:

$$\frac{dV}{dt} = dx.dy.\frac{d\eta}{dt} \tag{4.18}$$

If the latter equation is substituted in eq.(4.17) and all terms are divided by $dx.dy$ we

find:

$$h\left(\frac{\partial u}{\partial x}+\frac{\partial v}{\partial y}\right)+\frac{\partial \eta}{\partial t}=0 \tag{4.19}$$

The latter equation should now be combined with eq. (4.11) where the third equation can be simplified as a hydrostatic approximation essentially telling us that a water column of η meters is responsible for a certain pressure p:

$$p = g.\rho.\eta \tag{4.20}$$

following the requirement that the pressure p is computed relative to a surface that doesn't experience a change in height. We get the horizontal pressure gradients:

$$\frac{-1}{\rho}\frac{\partial p}{\partial x}=\frac{\partial(-g\eta)}{\partial x} \quad \text{and} \quad \frac{-1}{\rho}\frac{\partial p}{\partial y}=\frac{\partial(-g\eta)}{\partial y} \tag{4.21}$$

Moreover for the forcing terms F_x and F_y in eq. (4.11) we substitute the horizontal gradients:

$$F_x=\frac{\partial U^a}{\partial x}+G_x \quad \text{and} \quad F_y=\frac{\partial U^a}{\partial y}+G_y \tag{4.22}$$

where U^a is the total tide generating potential and G_x and G_y terms as a result of advection and/or friction. Substitution of eqns. (4.21) and (4.22) in eqn. (4.11) and elimination of the term $2\Omega\cos(\phi)w$ in the first and second equation results in a set of equations which were first formulated by Laplace:

$$\begin{aligned}
\frac{D\,u}{D\,t} &= \frac{\partial}{\partial x}\left(-g\eta+U^a\right)+f.v+G_x \\
\frac{D\,v}{D\,t} &= \frac{\partial}{\partial y}\left(-g\eta+U^a\right)-f.u+G_y \\
\frac{D\,\eta}{D\,t} &= -h\left(\frac{\partial u}{\partial x}+\frac{\partial v}{\partial y}\right)
\end{aligned} \tag{4.23}$$

The Laplace tidal equations consist of two parts; equations (4.23)(a-b) are called the momentum equations, and (4.23)(c) is called the continuity equation. Various refinements are possible, two relevant refinements are:

- We have ignored the effect of secondary tide potentials caused by ocean tides loading on the lithosphere, more details can be found in chapter 6.
- The depth term h could by replaced by $h+\eta$ because the ocean depth is increased by the water level variation η (although this modification would introduce a non-linearity).
- For the LTE: $\eta \ll h$.

To solve the LTE it is also necessary to pose initial and boundary conditions including a domain in which the equations are to be solved. From physical point of view a no-flux boundary condition is justified, in which case $(\overline{u},\overline{n})=0$ with $\overline{n}$ perpendicular to the boundary of the domain. For a global tide problem the domain is essentially the oceans, and the boundary is therefor the shore.

Other possibilities are to define a half open tide problem where a part of the boundary is on the open ocean where water levels are prescribed while another part is closed on the shore. This option is often used in civil engineering application where it is intended to study a limited area problem. Other variants of boundary conditions including reflecting or (weakly) absorbing boundaries are an option in some software packages.

In the next section we show simple solutions for the Laplace tidal equations demonstrating that the depth averaged velocity problem, better known as the barotropic tide problem, can be approximated by a Helmholtz equation which is characteristic for wave phenomena in physics.

4.4 Helmholtz equation

Intuitively we always assumed that ocean tides are periodic phenomena, but of course it would be nicer to show under which conditions this is the case. Let us introduce a test solution for the problem where we assume that:

$$u(t) = \hat{u}\exp(j\omega t) \tag{4.24}$$
$$v(t) = \hat{v}\exp(j\omega t) \tag{4.25}$$
$$\eta(t) = \hat{\eta}\exp(j\omega t) \tag{4.26}$$

where $j = \sqrt{-1}$. For tides we know that the gradient of the tide generating potential is:

$$U^a(t) = \hat{\Gamma}\exp(j\omega t) \tag{4.27}$$

Furthermore we will simplify advection and friction and assume that these terms can be approximated by:

$$G_x(t) = \hat{G}_x\exp(j\omega t) \tag{4.28}$$
$$G_y(t) = \hat{G}_y\exp(j\omega t) \tag{4.29}$$

If this test solution is substituted in the momentum equations then we obtain:

$$\begin{bmatrix} j\omega & -f \\ +f & j\omega \end{bmatrix}\begin{bmatrix} \hat{u} \\ \hat{v} \end{bmatrix} = -g\begin{bmatrix} \partial\hat{\eta}/\partial x \\ \partial\hat{\eta}/\partial y \end{bmatrix} + \begin{bmatrix} \partial\hat{\Gamma}/\partial x \\ \partial\hat{\Gamma}/\partial y \end{bmatrix} + \begin{bmatrix} G_x \\ G_y \end{bmatrix} \tag{4.30}$$

Provided that we are dealing with a regular system of equations it is possible to solve $\hat{u}$ and $\hat{v}$ and to substitute this solution in the continuity equation that is part of the LTE. After some manipulation we get:

$$(\omega^2 - f^2)\hat{\eta} + gh\left(\frac{\partial^2\hat{\eta}}{\partial x^2} + \frac{\partial^2\hat{\eta}}{\partial y^2}\right) = h\left(\frac{\partial^2\hat{\Gamma}}{\partial x^2} + \frac{\partial^2\hat{\Gamma}}{\partial y^2}\right) + h\left(\frac{\partial\hat{G}_x}{\partial x} + \frac{\partial\hat{G}_y}{\partial y}\right) + \frac{jfh}{\omega}\left(\frac{\partial\hat{G}_x}{\partial y} - \frac{\partial\hat{G}_y}{\partial x}\right) \tag{4.31}$$

The left hand side of equation (4.31) is known as the Helmholtz equation which is typical for wave phenomena in physics. The term gh in eq. (4.31) contains the squared surface speed (c) of a tidal wave. Some examples are: a tidal wave in a sea of 50 meter depth runs with a velocity of $\sqrt{50.g}$ which is about 22 m/s or 81 km/h. In an ocean of 5 km depth c will rapidly increase, we get 223.61 m/s or 805 km/h which is equal to that of

an aircraft. A critical step in the derivation of the Helmholtz equation is the treatment of advection and friction term contained in G_x and G_y and the vorticity term ζ. As long as these terms are written in the form of harmonic test functions like in (4.28) and (4.29) there is no real point of concern. To understand this issue we must address the problem of a drag law that controls the dissipation of a tidal wave.

4.5 Drag laws

The drag law is an essential component of a hydrodynamic tide model, omission of a dissipative mechanism results in modeling tides as an undamped system since tidal waves can not lose their energy. Physically seen this is completely impossible because the tides are continuously excited by gravitational forcing. A critical step is therefor the formulation of a dissipative mechanism which is often chosen as a bottom friction term. Friction between layers of fluid was initially considered to be too small to explain the dissipation problem in tides, friction against the walls of a channel or better the ocean floor is considered to be more realistic. In this way the ocean tides dissipate more than 75 percent of their energy, more details are provided in chapter 8.

There is an empirical law for bottom drag which was found by the Frenchman Chezy who found that drag is proportional to the velocity squared and inverse proportional to the depth of a channel. Chezy essentially compared the height gradient of rivers against the flow in the river and geology of the river bed. Under such conditions the river bed drag has to match the horizontal component of the pressure gradient, which essentially follows from the height gradient of the river. The Chezy law extended to two dimensions is:

$$G_x = -C_d u\sqrt{u^2+v^2} \tag{4.32}$$

$$G_y = -C_d v\sqrt{u^2+v^2} \tag{4.33}$$

where $C_d = g/(hC_z^2)$, g is gravity, h is depth and C_z a scaling coefficient, or the Chezy coefficient. In reality C_z depends on the physical properties of the river bed; reasonable values are between 40 and 70.

Fortunately there exist linear approximations of the Chezy law to ensure that the amount of energy dissipated by bottom friction over a tidal cycles obtains the same rate as the quadratic law. This problem was originally investigated by the Dutch physicist Lorentz. A realistic linear approximation of the quadratic bottom drag is for instance:

$$G_x = -ru/h \tag{4.34}$$

$$G_y = -rv/h \tag{4.35}$$

where r is a properly chosen constant (typically r=0.0013). Lorentz assumed that the linear and quadratic drag laws have to match, ie. predict the same loss of energy over 1 tidal cycle. Lorentz worked out this problem for the M_2 tide in the Waddenzee.

4.6 Linear and non-linear tides

We will summarize the consequences of non-linear acceleration terms that appear in the Laplace tidal equations:

- Linear ocean tides follow from the solution of the Laplace tidal equations whereby all forcing terms, dissipative terms and friction terms can be approximated as harmonic functions. The solution has to fulfill the condition posed by the Helmholtz equation, meaning that the tides become a wave solution that satisfies the boundary conditions of the Helmholtz equation. Essentially this means that ocean tides forced at a frequency ω result in a membrane solution oscillating at frequency ω. The surface speed of the tide is then $\sqrt{gH}$.

- Non-linear ocean tides occur when there are significant deviations from a linear approximation of the bottom drag law, or when the tide is forced through its basin geometry along the shore or through a channel. In this case advection and bottom friction are the main causes for the generation of so-called parasitic frequencies which manifest themselves as undertones, overtones or cross-products of the linear tide. Examples of non-linear tides are for instance M_0 and M_4 which are the result of an advective term acting on M_2. Some examples of cross-products are MS_0 and MS_4 which are compound tides as a result of M_2 and S_2.

4.7 Dispersion relation

Another way to look at the tide problem (or in fact many other wave problems in physics) is to study a dispersion relation. We will do this for the simplest case in order to demonstrate another basic property of ocean tides, namely that the decrease in the surface speed c causes a shortening of length scale of the wave. For the dispersion relation we assume an unforced or free wave of the following form:

$$u(x,y,t) = \hat{u}\exp(j(\omega t - kx - ly)) \tag{4.36}$$
$$v(x,y,t) = \hat{v}\exp(j(\omega t - kx - ly)) \tag{4.37}$$
$$\eta(x,y,t) = \hat{\eta}\exp(j(\omega t - kx - ly)) \tag{4.38}$$

which is only defined for a local region. This generic solution is that of a surface wave, ω is the angular velocity of the tide, and k and l are wave numbers that provide length scale and direction of the wave.

To derive the dispersion relation we ignore the right hand side of eq. (4.31) and substitute characteristic wave functions. This substitution results in:

$$(\omega^2 - f^2) = c^2\left(k^2 + l^2\right) \tag{4.39}$$

which is a surprisingly simple relation showing that k^2+l^2 has to increase when c decreases and visa versa. In other words, now we have shown that tidal wave lengths become shorter in shallow waters. The effect is demonstrated in figure 4.6 with a map of the tidal amplitudes and phases of the M_2 tide in the North Sea basin.

But, there are more hidden features in the dispersion relation. The right hand side of equation (4.39) is always positive since we only see squares of c, k and l. The left hand side is only valid when ω is greater than f. Please remember that the Coriolis parameter $f = 2\Omega\sin\phi$ is latitude dependent with zero at the equator. Near the equator we will always get free waves passing from west to east or visa versa.

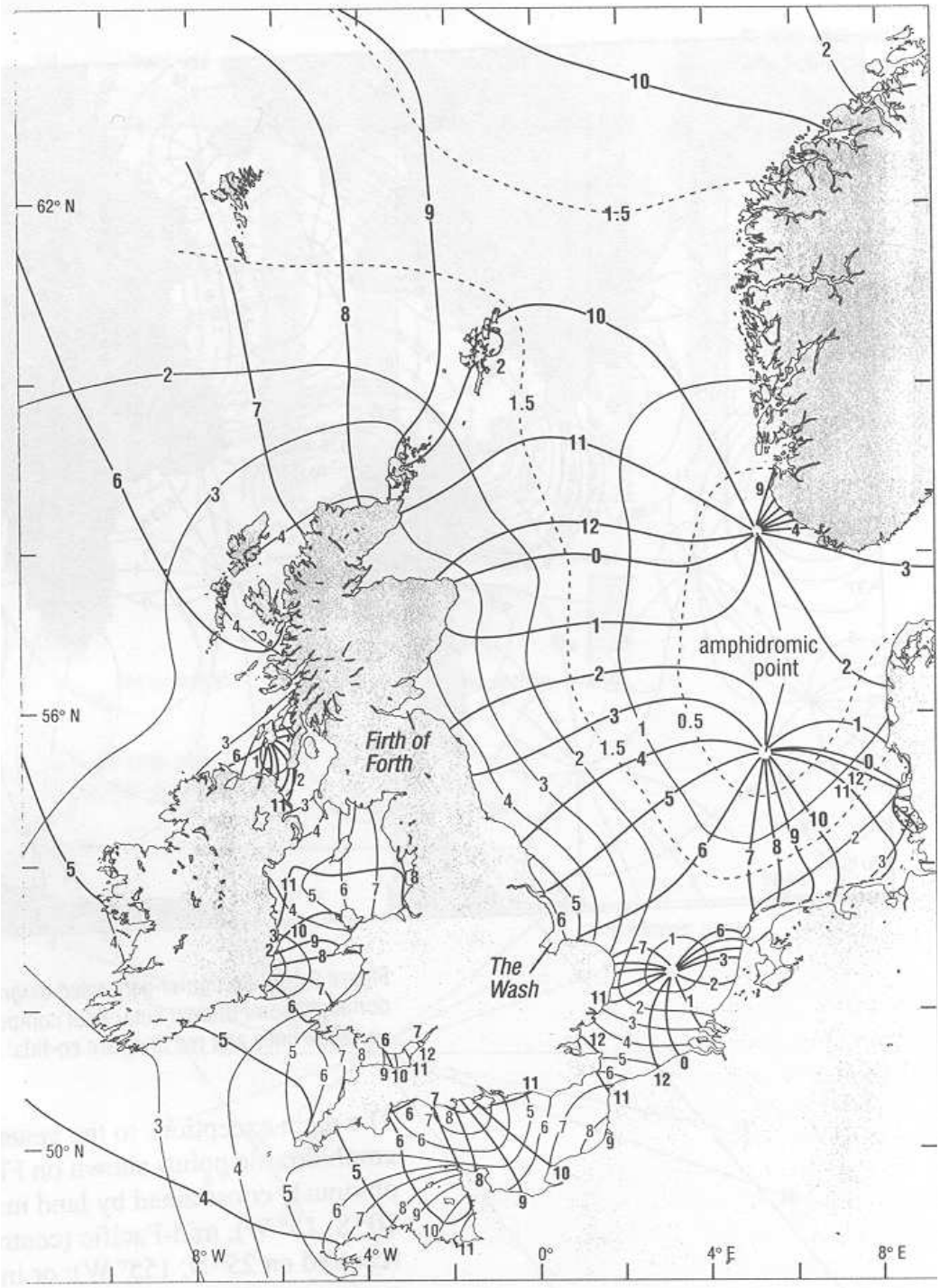

Figure 4.6: North Sea M2 tide

For frequencies ω equal to f one expects that there is a latitude band inside which the free wave may exist. A nice example is the K_1 tidal wave which is a dominant diurnal tide with a period of 23 hours and 56 minutes, so that $\omega = \Omega$. The conclusion is that free waves at the K_1 frequency can only exist when $\sin\phi$ is less than $1/2$ which is true for a latitudes between 30N and 30S.

4.8 Exercises

- What is the magnitude of the Coriolis effect for a ship sailing southward at 50N with a speed of 20 knots
- Is water flowing from your tap into the kitchen sink turbulent?
- What is the magnitude of a height gradient of a river with a flow of 0.5 m/s and a Chezy coefficient of 30. The mean depth of the river is 5 meter.
- What latitude extremes can we expect for free tidal waves at the M_m frequency?
- How much later is the tide at Firth of Worth compared to The Wash?
- What extra terms appear in the Helmholtz equation for a linear bottom drag model.
- Show that advection can be written as $\overline{u}\nabla\overline{u}$
- Shows that vorticity is conserved in fluid mechanics problems that are free of friction.

Chapter 5

Data analysis methods

Deep ocean tides are known to respond at frequencies identical to the Doodson numbers in tables B.1 and B.2. Non-linearities and friction in general do cause overtones and mixed tides, but, this effect will only appear in shallow waters or at the boundary of the domain. In the deep oceans it is very unlikely that such effects dominate in the dynamical equations. Starting with the property of the tides we present two well known data analysis methods used in tidal research.

5.1 Harmonic Analysis methods

A perhaps unexpected consequence of the tidal harmonics table is that at least 18.61 years of data would be required to separate two neighboring frequencies because of the fact that main lines in the spectrum are modulated by smaller, but significant, side-lines. Compare for instance table B.1 and B.2 where one can see that most spectral lines require at least 18.61 years of observation data in order to separate them from side-lines. Fortunately, extensive analysis conducted by [6] have shown that a smooth response of the sea level is likely. Therefore the more practical approach is to take at least two Doodson numbers and to form an expression where only a year worth of observations determine "amplitude and phase" of a constituent. However, this is only possible if one assumes a fixed *amplitude ratio* of a side-line with respect to a main-line where the ratio itself can be taken from the table of tidal harmonics.

Consider for instance table B.2 where M_2 is dominated by spectral lines at the Doodson numbers 255.555 and 255.545 and where the ratio of the amplitudes is approximately $-0.02358/0.63194 = -0.03731$. We will now seek an expression to model the M_2 constituent:

$$M_2(t) = C_{M_2}\left[\cos(2\omega_1 t - \theta_{M_2}) + \alpha\cos(2\omega_1 t + \omega_5 t - \theta_{M_2})\right] \tag{5.1}$$

where C_{M_2} and θ_{M_2} represent the amplitude and phase of the M_2 tide and where $\alpha = -0.03731$. Starting with:

$$\begin{aligned} M_2(t) &= C_{M_2}\cos(2\omega_1 t - \theta_{M_2}) \\ &+ \alpha C_{M_2}\{\cos(2\omega_1 t - \theta_{M_2})\cos(\omega_5 t) - \sin(2\omega_1 t - \theta_{M_2})\sin(\omega_5 t)\} \end{aligned}$$

we arrive at:

$$M_2(t) = C_{M_2}\left\{(1 + \alpha\cos(\omega_5 t))\cos(2\omega_1 t - \theta_{M_2}) - \alpha\sin(\omega_5 t)\sin(2\omega_1 t - \theta_{M_2})\right\} \tag{5.2}$$

which we will write as:

$$M_2(t) = C_{M_2} f(t) \left\{ \cos(u(t)) \cos(2\omega_1 t - \theta_{M_2}) - \sin(u(t)) \sin(2\omega_1 t - \theta_{M_2}) \right\} \tag{5.3}$$

or

$$M_2(t) = C_{M_2} f(t) \cos(2\omega_1 t + u(t) - \theta_{M_2}) \tag{5.4}$$

so that:

$$M_2(t) = A_{M_2} f(t) \cos(2\omega_1 t + u(t)) + B_{M_2} f(t) \sin(2\omega_1 t + u(t)) \tag{5.5}$$

where

$$\begin{aligned} A_{M_2} &= C_{M_2} \cos(\theta_{M_2}) \\ B_{M_2} &= C_{M_2} \sin(\theta_{M_2}) \end{aligned}$$

In literature the terms A_{M_2} and B_{M_2} are called "in-phase" and "quadrature" or "out-of-phase" coefficients of a tidal constituent, whereas the $f(t)$ and $u(t)$ coefficients are known as nodal modulation factors, stemming from the fact that $\omega_5 t$ corresponds to the right ascension of the ascending node of the lunar orbit. In order to get convenient equations we work out the following system of equations: ($\Omega = \omega_5 t$):

$$\begin{aligned} f(t) &= \left\{ (1 + \alpha \cos(\Omega))^2 + (\alpha \sin(\Omega))^2 \right\}^{1/2} \\ u(t) &= \arctan\left(\frac{\alpha \sin(\Omega)}{1 + \alpha \cos(\Omega)} \right) \end{aligned}$$

Finally a Taylor series around $\alpha = 0$ gives:

$$\begin{aligned} f(t) &= (1 + \frac{1}{4}\alpha^2 + \frac{1}{64}\alpha^4) + (\alpha - \frac{1}{8}\alpha^3 - \frac{1}{64}\alpha^5) \cos\Omega \\ &+ (-\frac{1}{4}\alpha^2 + \frac{1}{16}\alpha^4) \cos(2\Omega) + (\frac{1}{8}\alpha^3 - \frac{5}{128}\alpha^5) \cos(3\Omega) \\ &- \left(\frac{5}{64}\right) \cos(4\Omega) + \frac{7\alpha^5}{128} \cos(5\Omega) + O(\alpha^6) \end{aligned} \tag{5.6}$$

$$\begin{aligned} u(t) &= \alpha \sin(\Omega) - \frac{1}{2}\alpha^2 \sin(2\Omega) + \frac{1}{3}\alpha^3 \sin(3\Omega) \\ &- \frac{1}{4}\alpha^4 \sin(4\Omega) + \frac{1}{5}\alpha^5 \sin(5\Omega) + O(\alpha^6) \end{aligned} \tag{5.7}$$

Since α is small it is possible to truncate these series at the quadratic term. The equations show that $f(t)$ and $u(t)$ are only slowly varying and that they only need to be computed once when e.g. working with a year worth of tide gauge data.

The Taylor series for the above mentioned nodal modulation factors were derived by means of the Maple software package and approximate the more exact expressions for f and u. However the technique seems to fail whenever increased ratios of the main line to the side line occur as is the case with the e.g. the K_2 constituent or whenever there are more side lines. A better way of finding the nodal modulation factors is then to numerically compute at sufficiently dense steps the values of the tide generating potential for a particular constituent at an arbitrary location on Earth over the full nodal cycle and to numerically estimate Fourier expressions like $f(\Omega) = \sum_n f_n \cos(n.\Omega)$ and $u(\Omega) = \sum_n u_n \sin(n.\Omega)$ with eq. (5.4) as a point of reference.

5.2 Response method

The findings of [6] indicate that ocean tides $\eta(t)$ can be predicted as a convolution of a smooth weight function and the tide generating potential U^a:

$$\hat{\eta}(t) = \sum_s w(s) U^a(t - \tau_s) \tag{5.8}$$

with the weights w determined so that the prediction error $\eta(t) - \hat{\eta}(t)$ is a minimum in the least squares sense. The weights $w(s)$ have a simple physical interpretation: they represent the sea level response at the port (read: point of observation) to a unit impulse $U^a(t) = \delta(t)$, hence the name "response method". The actual input function $U^a(t)$ may be regarded as a sequence of such impulses. The scheme used in [6] is to expand $U^a(t)$ in spherical harmonics,

$$U^a(\theta, \lambda; t) = g \sum_{n=0}^{N} \sum_{m=0}^{n} [a_{nm}(t) U_{nm}(\theta, \lambda) + b_{nm}(t) V_{nm}(\theta, \lambda)] \tag{5.9}$$

containing the complex spherical harmonics:

$$U_{nm} + jV_{nm} = Y_{nm} = (-1)^m \left[\frac{2n+1}{4\pi}\right]^{1/2} \left[\frac{(n-m)!}{(n+m)!}\right]^{1/2} P_{nm}(\cos\theta) \exp(jm\lambda) \tag{5.10}$$

and to compute the coefficients $a_{nm}(t)$ and $b_{nm}(t)$ for the desired time interval. The convergence of the spherical harmonics is rapid and just a few terms n, m will do. The m-values separate input functions according to species and the prediction formalism is:

$$\hat{\eta}(t) = \sum_{n,m} \sum_s [u_{nm}(s) a_{nm}(t - \tau_s) + v_{nm}(s) b_{nm}(t - \tau_s)] \tag{5.11}$$

where the prediction weights $w_{nm}(s) = u_{nm}(s) + jv_{nm}(s)$ are determined by least-squares methods, and tabulated for each port (these take the place of the tabulated C_k and θ_k in the harmonic method). For each year the global tide function $c_{nm}(t) = a_{nm}(t) + jb_{nm}(t)$ is computed and the tides then predicted by forming weighted sums of c using the weights w appropriate to each port. The spectra of the numerically generated time series $c(t)$ have all the complexity of the Darwin-Doodson expansion; but there is no need for carrying out this expansion, as the series $c(t)$ serves as direct input into the convolution prediction. There is no need to set a lower bound on spectral lines; all lines are taken into account in an optimum sense. There is no need for the f, u factors, for the nodal variations (and even the 20926 y variation) is already built into $c(t)$. In this way the response method makes explicit and general what the harmonic method does anyway – in the process of applying the f, u factors. The response method leads to a more systematic procedure, better adapted to computer use. According to [6] its formalism is readily extended to include nonlinear, and perhaps even meteorological effects.

5.3 Exercises

1. Why is the response method for tidal analysis more useful and successful than the harmonic tidal analysis method, ie. what do we learn from this method what couldn't be seen with the harmonic tide analysis method.

2. Design a flow diagram for a program that solves tidal amplitudes and phases from a dataset of tide gauge readings that contains gaps and biases. Basic linear algebra operations such as a matrix inversion should not be worked out in this flow diagram.

3. How could you see from historic tide constants at a gauge that the local morphology has changed over time near the tide gauge.

Chapter 6

Load tides

6.1 Introduction

Any tide in the ocean will load the sea floor which is not a rigid body. One additional meter of water will cause 1000 kg of mass per square meter; integrated over a 100 by 100 km sea we are suddenly dealing 10^{13} kg which is a lot of mass resting on the sea floor. Loading is a geophysical phenomenon that is not unique to tides, any mass that rests on the lithosphere will cause a loading effect. Atmospheric pressure variations, rainfall, melting of land ice and evaporation of lakes cause similar phenomena. An important difference is whether we are dealing with a visco-eleastic or just an elastic process. This discussion is mostly related to the time scales at which the phenomenon is considered. For tides we only deal with elastic loading. The consequence is that the Earth's surface will deform, and that the deformation pattern extends beyond the point where the original load occurred. In order to explain the load of a unit point mass we introduce the Green function concept, to model the loading effect of a surface mass layer we need a convolution model, a more efficient algorithm uses spherical harmonics, a proof is presented in the last section of this chapter.

6.2 Green functions

In [27] it is explained that a unit mass will cause a geometric displacement at a distance ψ from the source:

$$G(\psi) = \frac{r_e}{M_e} \sum_{n=0}^{\infty} h'_n P_n(\cos\psi) \tag{6.1}$$

where M_e is the mass of the Earth and r_e its radius. The Green function coefficients h'_n come from a geophysical Earth model, two versions are shown in table 6.1. The geophysical theory from which these coefficients originate is not discussed in these lectures, instead we mention that they represent the elastic loading effect and not the visco-elastic effect.

6.3 Loading of a surface mass layer

Ocean load tides cause vertical displacements of geodetic stations away from the load as has been demonstrated by analysis of GPS and VLBI observations near the coast where

		Farrell		Pagiatakis	
n	α_n	$-h'_n$	$-k'_n$	$-h'_n$	$-k'_n$
1	0.1876	0.290	0	0.295	0
2	0.1126	1.001	0.308	1.007	0.309
3	0.0804	1.052	0.195	1.065	0.199
4	0.0625	1.053	0.132	1.069	0.136
5	0.0512	1.088	0.103	1.103	0.103
6	0.0433	1.147	0.089	1.164	0.093
8	0.0331	1.291	0.076	1.313	0.079
10	0.0268	1.433	0.068	1.460	0.074
18	0.0152	1.893	0.053	1.952	0.057
30	0.0092	2.320*	0.040*	2.411	0.043
50	0.0056	2.700*	0.028*	2.777	0.030
100	0.0028	3.058	0.015	3.127	0.016

Table 6.1: Factors α_n in equation (6.3), and the loading Love numbers computed by [27] and by [24]. An asterisk $(*)$ means that data was interpolated at $n = 32, 56$

vertical twice daily movements can be as large as several centimeters, see for example figure 6.1. In order to compute these maps it is necessary to compute a convolution integral where a surface mass layer, here in the form of an ocean tide chart, is multiplied times Green's functions of angular distance from each incremental tidal load, effective up to 180°. The loading effect is thus computed as:

$$\eta_l(\theta, \lambda, t) = \int_\Omega G(\psi) d\, M(\theta', \lambda', t) \tag{6.2}$$

where $d\,M$ represents the mass at a distance ψ from the load. This distance ψ is the spherical distance between (ϕ, λ) and (ϕ', λ'). There is no convolution other than in ϕ and λ, the model describes an instantaneous elastic response.

6.4 Computing the load tide with spherical harmonic functions

But given global definition of the ocean tide η it is more convenient to express it in terms of a sequence of load-Love numbers k'_n and h'_n times the spherical harmonics of degree n of the ocean tide. If $\eta_n(\theta, \lambda; t)$ denote any n^{th} degree spherical harmonics of the tidal height η, the secondary potential and the bottom displacement due to elastic loading are $g(1 + k'_n)\alpha_n\eta_n$ and $h'_n\alpha_n\eta_n$ respectively where:

$$\alpha_n = \frac{3}{(2n+1)} \times \frac{\rho_w}{\rho_e} = \frac{0.563}{(2n+1)} \tag{6.3}$$

where ρ_w is the mean density of water and ρ_e the mean density of Earth. (Appendix A provides all required mathematical background to derive the above expression, this result

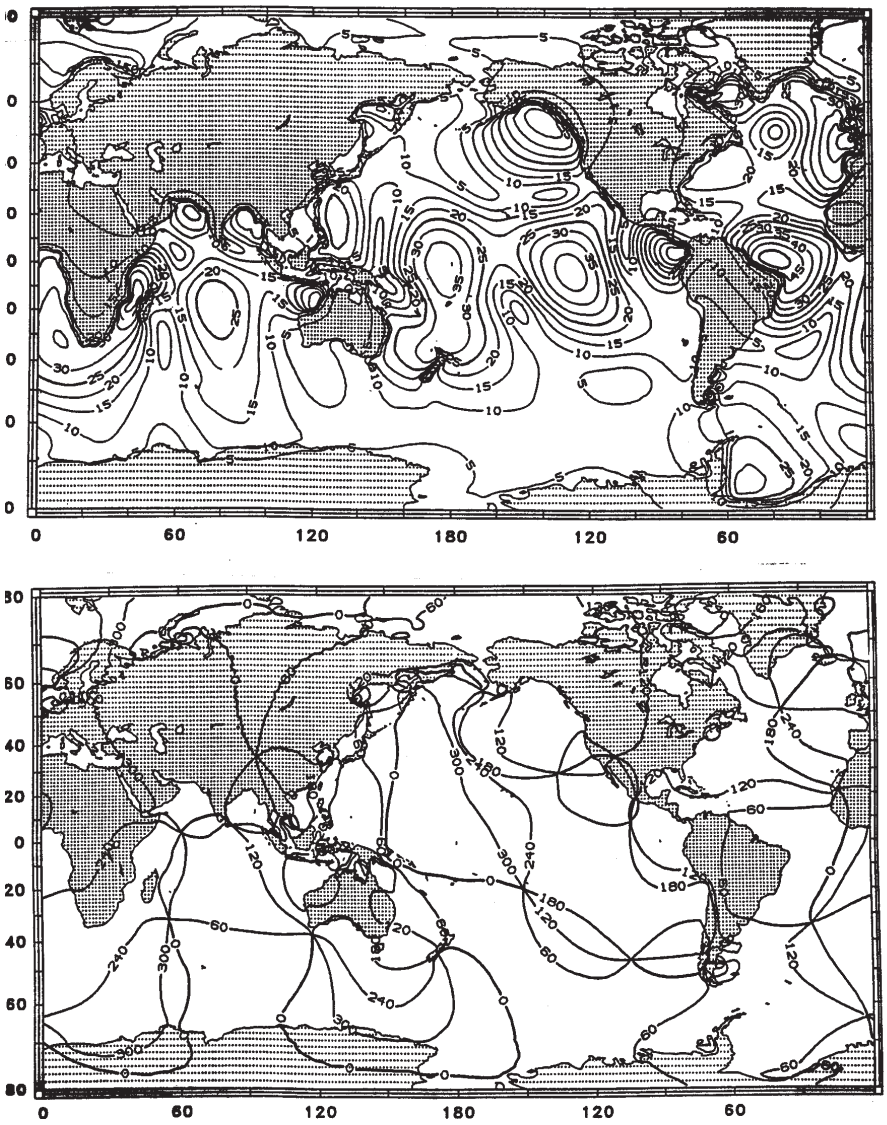

Figure 6.1: The top panel shows the amplitude map in millimeters of the M_2 load tide, the bottom panel shows the corresponding phase map. Note that the load tide extends beyond the oceanic regions and that the lithosphere also deforms near the coast.

follows from the convolution integral on the sphere that is evaluated with the help of spherical harmonics) The essential difference from the formulation of the body tide is that the spherical harmonic expansion of the ocean tide itself requires terms up to very high degree n, for adequate definition. Farrell's (1972) calculations of the load Love numbers, based on the Gutenberg-Bullen Earth model, are frequently used. Table 6.1 is taken from [4] and lists a selection of both Farrell's numbers and those from a more advanced calculation by [24], based on the PREM model.

Why is it so efficient to consider a spherical harmonic development of the ocean tide maps? Here we refer to the in-phase or quadrature components of the tide which are both treated in the same way. The reason is that convolution integrals in the spatial domain can be solved by multiplication of Green functions coefficients and spherical harmonic coefficients in the spectral domain. The in-phase or quadrature ocean load tide maps contained in $H(\theta, \lambda)$ follow then from a convolution on the sphere of the Green function $G(\psi)$ and an in-phase or quadrature ocean tide height function contained in $F(\theta, \lambda)$, for details see appendix A.

6.5 Exercises

1. Explain how you would compute the self attraction tide signal provided that the ocean tide signal is provided.

2. How do you compute the vertical geometric load at the center of a cylinder with a radius of ψ degrees.

3. Design a Green function to correct observed gravity values for the presence of mountains and valleys, i.e. that corrects for a terrain effect. Implement this Green function in a method that applies the correction.

Chapter 7

Altimetry and tides

7.1 Introduction

Satellite altimetry is nowadays an accurate technique whereby height profiles are measured along satellite tracks over the ocean. Repeated measurement of these height profiles followed by a suitable data analysis method provides in principle estimates of the altimetric tide. One problem is that an altimeter will observe the sum of the solid Earth tide, an oceanic tide and a load tide. The solid Earth tide can be modelled when the Love numbers h_n are provided. Separating the load tide from the ocean tide requires one to solve an integral equation. In this chapter we will discuss both issues.

7.2 Aliasing

Tides observed by a satellite altimeter are usually systematically under sampled. The under sampled diurnal and semi-diurnal frequencies result in alias periods significantly longer than the natural periods of the tides. Any altimeter satellite has been plagued by this problem, SEASAT's lifetime (NASA altimeter, 1978) was too short for doing any serious tidal analysis, GEOSAT (US Navy altimeter, 1985-1990) had several problems among which that the M_2 tide aliases to a period of about a year and finally ERS-1 (ESA altimeter 1991-1996) is by definition not suited for tidal research because the sun-synchronous orbit causes all solar tides to be sampled at the same phase.

7.3 Separating ocean tide and load tides

A satellite altimeter will observe the sum of an ocean and a load tide, where the latter is obtained by convolution with respect to the ocean tide, thus we have:

$$S_a = S_o + L(S_o) \tag{7.1}$$

where S_a is the tide observed by the altimeter, and where S_o is a ocean tide. Operator $L()$ is a convolution integral as explained in chapter 6. In order to obtain ocean and load tides we have to solve an integral equation. Since L is a linear operator the ocean tide is obtained by:

$$S_o = (I + L)^{-1} S_a \tag{7.2}$$

It turns out that there is a fast inversion algorithm capable of inverting this problem within several iterations

$$\begin{aligned} S_l^{(0)} &= L(S_a) \\ S_o^{(0)} &= S_a - S_l^{(0)} \\ S_l^{(1)} &= L(S_o^{(0)}) \\ S_o^{(1)} &= S_a - S_l^{(1)} \\ S_l^{(2)} &= L(S_o^{(1)}) \\ S_o^{(2)} &= S_a - S_l^{(2)} \\ &\vdots \end{aligned}$$

This procedure has been used to separate the ocean and load tide from TOPEX/Poseidon altimetry data.

7.4 Results

To close this chapter on tides we want to mention that the TOPEX/POSEIDON satellite altimeter mission (NASA/CNES, active since August 1993) has stimulated the development of a series of new tide models more accurate than any previous global hydrodynamic model, see for instance [7]. The main reason for the success of the Topex/Poseidon mission in modeling the *deep* ocean tides should be seen in the context of the design of the mission where the choice of the nominal orbit is such that all main tidal constituents alias to relatively short periods. A few of the results are tabulated in table 7.1 where the r.m.s. comparisons to 102 "ground-truth" stations in (cm) are shown. Ocean tides in shallow coastal areas are not that easily observed with Topex/Poseidon altimetry because of the non-harmonic response of tides in shallow seas leading to spatial details exceeding the resolution attainable by the Topex/Poseidon inter track spacing. This behavior was explained in chapter 4, in particular at the point where the dispersion relation of barotropic waves was discussed. For shallow seas it is in general better to rely on regional tide/storm surge models. An example for the North Sea area is the Continental Shelf Model (CSM) maintained by the RIKZ group, Department of Rijkswaterstaat, Koningskade 4, 2500 EX Den Haag, The Netherlands.

7.5 Exercises

1. Show that the recursive algorithm to solve eq. (7.2) is valid.

2. What is the aliasing period of the M_2 tide when it is observed from the Envisat orbit which is a 35 day sun-synchronous repeat orbit. Can you also observe the S_2 tide with an altimeter from this orbit?

3. The T/P orbit completes 127 orbital periods in 10 nodal days. Use the J_2 gravity precession equations to find the proper orbital altitude at an inclination of 66 degrees and an eccentricity of 0.001. What is the ground track repeat time.

Authors	version	Q_1	O_1	P_1	K_1	N_2	M_2	S_2	K_2
Schwiderski	1980	0.34	1.23	0.61	1.44	1.19	3.84	1.66	0.59
Cartwright-Ray	1991		1.22	0.63	1.89	0.96	3.23	2.22	
Le Provost et al.	meom94.1	0.28	1.04	0.46	1.23	0.87	2.99	1.56	0.50
Egbert et al.	tpxo.1		0.96		1.26		2.30	1.55	
Egbert et al.	tpxo.2	0.29	0.98	0.45	1.32	0.76	2.27	1.26	0.56
Sanchez-Pavlis	gsfc94a	0.35	1.06	0.54	1.41	0.86	2.31	1.23	0.66
Ray et al.	1994	0.37	1.00	0.40	1.25	0.81	2.04	1.23	0.51
Schrama-Ray	1993.10		1.15		1.35		2.02	1.26	
Schrama-Ray	1994.11		1.02		1.19	0.85	1.85	1.20	

Table 7.1: Ground truth comparison at 102 tide gauges, the first two tide models are developed before Topex/Poseidon. Le Provost et al. ran a global finite element model that is free from Topex/Poseidon data. Egbert et al., also ran a finite element model while assimilating Topex/Poseidon data. Sanchez & Pavlis and Ray et al. used so-called Proudman functions to model the tides, they did incorporate Topex/Poseidon data. Schrama & Ray applied a straightforward harmonic analysis to the Topex/Poseidon data to determine improvements with respect to a number of tidal constituents.

4. Use the answers of the previous question to compute the aliasing period of the M_2 and the S_2 tide.

5. How much time does it take to disentangle Ssa and K_1 from T/P.

Chapter 8

Tidal Energy Dissipation

8.1 Introduction

This chapter contains background information on energy computations that apply to ocean tides. The subject of tidal energy dissipation is known for quite some time, a comprehensive reference is [16] where the problem is reviewed from a point of view prior to the refinement of tidal models by TOPEX/POSEIDON altimetry, see [7] [23]. Dissipation means that potential and kinetic energy in the ocean tides is converted into another form of energy. Where this process actually occurs and into which form energy is converted are separate questions.

Basic observations confirming that energy is dissipated in oceanic tides are linked to the slowdown of Earth rotation, which is about $-5 \times 10^{-22}\text{rad/s}^{-2}$, and lengthening of the distance between the Earth and the Moon by about 3.82 ± 0.07 cm/year, see also [8], [29], [28] and [16]. The Earth Moon configuration is shown in figure 8.1: According to [28] the total rate of dissipation due to the Moon is thereby constrained at 3 TW. If we add the solar tides then the total dissipation becomes 4 TW. For the M_2 tide the dissipation is 2.50 ± 0.05 Terrawatts (TW), see also [8]. In [28] it is suggested that the 2.5 TW is partially dissipated into body tides by 0.1 TW (according to [22]) and that the remaining 2.4 TW is dissipated in the oceans. For most part this remainder is dissipated by friction in shallow waters while another part goes into internal wave generation. In [14] one finds an estimate of 0.7 TW of energy dissipation in the deep oceans at the M_2 tide which is mainly attributed to internal wave generation at sub-surface ridges and at continental shelf boundaries. The relevance of energy dissipation in the deep oceans is that it is partly responsible for maintenance of the observed abyssal density stratification. The required energy to maintain this stratification involves mixing for which [30] estimates that 2 TW is required. The internal tides are according to [14] now responsible for approximately 1 TW in this process, the remaining part is due to wind effects.

The problem of sketching a complete picture of the dissipation mechanisms is clearly a multidisciplinary scientific challenge where astronomy, geodesy, physical oceanography and meteorology come together. Purpose of writing this chapter is to go through the derivation of the tidal energy equations and to confirm the global dissipation rates in the oceanic tides from a handful of existing models. We start with the equations of motion and show the necessary steps to arrive at the energy equation which contain a work term,

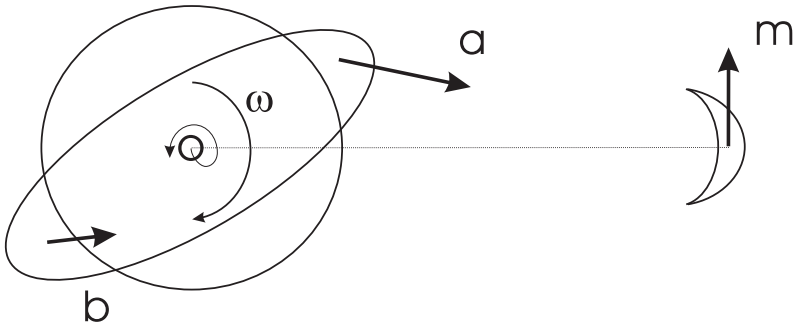

Figure 8.1: In this figure it is shown why the Earth spin rate is slowing down as a result of the gravitational torque formed by the acceleration vectors a and b. The Moon is also slowed down by this torque, causing it to move into a direction away from Earth.

a divergence term and a dissipation term. We will integrate this equation over a tidal cycle and over the oceans to confirm that the dissipation term equals the work term. In an example we demonstrate that the global dissipation rate at M_2 is 2.41 TW for the GOT99.2 model cf. [23]. The dissipation rates for other waves such as O_1 K_1 and S_2 are smaller; they are respectively 0.17, 0.33 and 0.43 TW.

The following sections discuss the problem of energy consideration in ocean tides (8.2) and results for the global tidal energy dissipation problem based upon several tide models (8.3).

8.2 Tidal energetics

We start with the equations of motion whereby the velocity terms $\overline{u}$ are averaged over a water column, see also [1] or eqns (4.23)(a-c):

$$\partial_t \overline{u} + \overline{f} \times \overline{u} = -g\nabla\eta + \nabla\Gamma - \overline{F} \tag{8.1}$$

$$\partial_t \eta = -\nabla.(\overline{u}H) \tag{8.2}$$

In these equations H is the height of the water column, η is the surface elevation, $\overline{f}$ is the Coriolis vector, g is the gravitational acceleration, $\nabla\Gamma$ is the acceleration term that sets water in motion and $\overline{F}$ contains terms that model the dissipation of energy or terms that model advection. Essentially the momentum equations (8.1) state that the Coriolis effect, local gravity and the gradient of the pressure field are balanced while the continuity equation (8.2) enforces that there are no additional drains and sources.

For tidal problems the forcing function Γ is a summation of harmonic functions depending on σ indicating the frequency of a tidal line. If $\overline{F}$ is linear, in the sense that we don't allow velocity squaring of $\overline{u}$ and η, while imposing harmonic boundary conditions at frequency σ then solutions for $\overline{u}$ and η will also take place at σ. However if $\overline{F}$ contains

advective or non-linear frictional terms both causing a velocity squaring effect then the equations become non-linear so that solutions of $\overline{u}$ and η will contain other frequencies being the sums of differences of individual tidal lines. By means of scaling considerations one can show, see [4], that such non-linearities only play a marginal role and that they are only significant in coastal seas. An example is the overtone of M_2 (called M_4) which is small in the open oceans, see also chapter 4.

In [2] we find that the energy equation is obtained by multiplying the momentum equations (8.1) times $\rho H\overline{u}$ and the continuity equation (8.2) times $g\rho\eta$ with ρ representing the mean density of sea water. (Unless it is mentioned otherwise we assume that $\rho = \rho_w$). As a result we obtain:

$$\partial_t \left(\frac{1}{2}\rho H(u^2 + v^2) + \frac{1}{2} g\rho\eta^2 \right) = -g\rho H \nabla . (\overline{u}\eta) + \rho H \overline{u} . \nabla\Gamma - \rho H \overline{u} . \overline{F} \tag{8.3}$$

where we used the property $\nabla (ab) = a\nabla b + b\nabla a$. In the following we evaluate the time average over a tidal period by integrating all terms in eq. (8.3) over a tidal period T where $T = 2\pi/\sigma$. In order to condense typesetting a new notation is introduced:

$$< F > = \frac{1}{T} \int_{t=c}^{t=T+c} F(t)\, dt$$

where we remind that:

$$< \partial_t \left(\frac{1}{2}\rho H(u^2 + v^2) + \frac{1}{2} g\rho\eta^2 \right) > = 0$$

due to the fact that $\overline{u} = (u, v)$ and η are harmonic functions. (Note: formally the continuity equation should contain a term $H + \eta$ instead of just H, yet $\eta \ll H$ so that the effect can be ignored in the computations.) Characteristic in the discussion of the tidal energy equation is that the averaging operator will not cancel the remaining terms in eq. (8.3). We obtain:

$$< W > + < P > = < D > \tag{8.4}$$

where $< W >$ is the gravitational input or work put into the tides:

$$< W > = \rho H < \overline{u} . \nabla\Gamma >$$

with $< P >$ denoting the divergence of energy flux with:

$$< P > = -g\rho H \nabla . < \overline{u}\, \eta >$$

The dissipation of energy $< D >$ is entirely due to $\overline{F}$:

$$< D > = \rho H < \overline{u} . \overline{F} >$$

To obtain the rate at which tidal energy is dissipated eq. (8.4) must be integrated locally over a patch of ocean or globally over the entire oceanic domain, see also [2] [4] [14] [16] [28].

8.2.1 A different formulation of the energy equation

Let η be the oceanic tide, η_e the equilibrium tide and η_{sal} the self-attraction and loading tide and $\overline{U}$ the volume transport then, cf. [14]:

$$< D >= -g\rho\nabla. < \overline{U}\eta > +g\rho < \overline{U}\nabla\eta_e > +g\rho < \overline{U}\nabla\eta_{sal} >$$

where $\overline{U} = H\overline{u}$ and

$$\eta_e = g^{-1}\sum_n (1 + k_n - h_n)U_n^a$$

with U_n^a denoting the astronomical tide potential and h_n and k_n Love numbers for the geometric radial deformation and the induced potential that accompanies this deformation. The self-attraction and loading tide η_{sal} is:

$$\eta_{sal} = g^{-1}\sum_{nma} (1 + k'_n - h'_n)\frac{3(\rho_w/\rho_e)}{(2n+1)}\eta_{nma}Y_{nma}(\theta,\lambda)$$

where ρ_e is the mean density of the Earth while h'_n and k'_n are loading Love numbers. In this equation η_{nma} are spherical harmonic coefficients of the ocean tide elevation field and $Y_{nma}(\theta,\lambda)$ spherical harmonic functions. To avoid confusion we mention that our normalization procedures are chosen such that:

$$\int_\Omega Y_{nma}^2(\theta,\lambda)\, d\Omega = 4\pi$$

where

$$Y_{nma}(\theta,\lambda) = \begin{cases} \cos(m\lambda)\overline{P}_{nm}(\cos\theta) & : \quad a = 0 \\ \sin(m\lambda)\overline{P}_{nm}(\cos\theta) & : \quad a = 1 \end{cases}$$

with λ and θ denoting the geographic longitude and co-latitude.

8.2.2 Integration over a surface

So far the tidal energy equation (8.4) applies to a local patch of ocean. If we are interested in a dissipation rate over a domain Ω then it is necessary to evaluate the surface integral. For the work integral we can use the property:

$$< \widehat{W} > \; = \; \int_\Omega \rho H < \overline{u}.\nabla\Gamma > d\,\Omega \; = \; \int_\Omega < \rho H\nabla.(\overline{u}\Gamma) > d\,\Omega - \int_\Omega < \rho H\Gamma\nabla.\overline{u} > d\,\Omega \quad (8.5)$$

where the continuity equation $\nabla.(\overline{u}H) = -\partial_t\eta$ applies to the second integral on the hand side. After integrating all terms we get:

$$< \widehat{W_1} > \; + \; < \widehat{W_2} > \; + \; < \widehat{P} > \; = \; < \widehat{D} > \quad (8.6)$$

where:

$$< \widehat{W_1} > \; = \; \int_\Omega < \rho\Gamma\frac{\partial\eta}{\partial t} > \, d\Omega \quad (8.7)$$

$$< \widehat{W_2} > \; = \; \int_\Omega < \rho\nabla.(H\overline{u}\Gamma) > \, d\Omega \quad (8.8)$$

$$<\widehat{P}> \;=\; \int_{\Omega} < -g\rho\nabla.(H\overline{u}\eta) > \; d\Omega \tag{8.9}$$

For completeness it should be mentioned that the surface integrals for $<\widehat{W_2}>$ and $<\widehat{P}>$ may be replaced by line integrals over an element ds along the boundary of Ω, cf. [2]:

$$<\widehat{W_2}> \;=\; \oint_{\partial\Omega} < \rho\,\Gamma\,H(\overline{u}.\overline{n}) > \; ds \tag{8.10}$$

and

$$<\widehat{P}> \;=\; \oint_{\partial\Omega} < -g\rho\,\eta\,H(\overline{u}.\overline{n}) > \; ds \tag{8.11}$$

where $\overline{n}$ is a vector perpendicular to $\partial\Omega$.

8.2.3 Global rate of energy dissipation

In case the global oceans are our integration domain we can assume that $<\widehat{W_2}> = 0$ and $<\widehat{P}> = 0$ since the corresponding surface integrals can be written as line integrals along the boundary $\partial\Omega$ where we know that the condition $(\overline{u}.\overline{n}) = 0$ applies. The conclusion is that the global dissipation rate can be derived by $<\widehat{D}> \;=\; <\widehat{W_1}>$, meaning that we only require knowledge of the function Γ and the ocean tide elevation field η.

Spherical harmonics

At this point it is convenient to switch to spherical harmonic representations of all relevant terms that are integrated in the work integral because of orthogonality properties, see also [16]. A convenient representation of the oceanic tidal elevation field η is a series of global grids whereby an in-phase and a quadrature version are provided for a selected number of waves in the diurnal and semi-diurnal frequency band. The problem of representing η can be found in [4] where it is shown that:

$$\eta(\theta,\lambda,t) = \sum_{\sigma} f_\sigma \left[P_\sigma(\theta,\lambda)\cos(\sigma(t) - u_\sigma) + Q_\sigma(\theta,\lambda)\sin(\sigma(t) - u_\sigma)\right] \tag{8.12}$$

The definitions of f_σ and u_σ are related to the effect of side lines modulating the main wave. In the following discussion we will ignore the effect of f_σ and u_σ (ie. $f_\sigma = 1$ and $u_\sigma = 0$) and assume that their contribution can be neglected in the evaluation of the energy equation. In essence this assumption says that we convert the formal definition of a tidal constituent into that of a single wave at frequency σ.

Prograde and retrograde waves

To appreciate the physics of tidal energy dissipation [16] presents a wave splitting method. The essence of this method is that we get prograde and retrograde waves which are constructed from the spherical harmonic coefficients of P_σ and Q_σ in eq. (8.12) at a given frequency σ. To retrieve both wave types we develop P_σ and Q_σ in spherical harmonics:

$$P_\sigma \;=\; \sum_{nm} \left[a_{nm}\cos m\lambda + b_{nm}\sin m\lambda\right]\overline{P}_{nm}(\cos\theta) \tag{8.13}$$

$$Q_\sigma \;=\; \sum_{nm} \left[c_{nm}\cos m\lambda + d_{nm}\sin m\lambda\right]\overline{P}_{nm}(\cos\theta) \tag{8.14}$$

to arrive at:

$$\eta(\theta,\lambda,t) = \sum_{nm\sigma} \left[D^{+}_{nm} \cos(\sigma(t) + m\lambda - \psi^{+}_{nm}) + D^{-}_{nm} \cos(\sigma(t) - m\lambda - \psi^{-}_{nm}) \right] \overline{P}_{nm}(\cos\theta) \tag{8.15}$$

with:

$$D^{\pm}_{nm} \cos(\psi^{\pm}_{nm}) = \frac{1}{2}(a_{nm} \mp d_{nm}) \tag{8.16}$$

$$D^{\pm}_{nm} \sin(\psi^{\pm}_{nm}) = \frac{1}{2}(c_{nm} \pm b_{nm}) \tag{8.17}$$

In this notation the wave selected with the + sign is prograde; it is a phase locked wave that leads the astronomical bulge with a certain phase lag. The second solution indicated with the − sign is a retrograde wave that will be ignored in further computations. From here on D^{+}_{nm} and ψ^{+}_{nm} are the only components that remain in the global work integral $< \widehat{W_1} >$.

Tables of spherical harmonic coefficients and associated prograde and retrograde amplitudes and phase lags exist for several ocean tide solutions, see also [23] who provides tables of 4 diurnal waves Q_1 O_1 P_1 K_1 and 4 semi-diurnal waves N_2 M_2 S_2 K_2. The required $D^{\pm}_{nm}$ and $\psi^{\pm}_{nm}$ terms are directly derived from the above equations, all be it that our spherical harmonic coefficients b_{nm} and d_{nm} come with a negative sign compared to [23].

Analytical expression for the global rate of dissipation

In the following we will apply the coefficients a_{nm} through d_{nm} in eqns. (8.13) and (8.14) in the evaluation of eq.(8.7). We require the time derivative of the tidal elevation field and the Γ function, a discussion of both terms and their substitution in eq.(8.7) is discussed below.

Forcing function

For the forcing function Γ we know that it is directly related to the astronomical tide generation function U^{a}_{n} and secondary potentials that follow from the self attraction and loading tide:

$$\Gamma = g\ (\eta_e + \eta_{sal}) \tag{8.18}$$

However from this point on we concentrate of the η_e term assuming that the η_{sal} term is smaller. The justification for the using $\Gamma = g\,\eta_e$ is that the an equilibrium ocean tide should be achieved in case there are no tidal currents $\overline{u}$ and terms $\overline{F}$, see also eq. (8.1). In addition we know from [4] that for all dominant tidal waves we always deal with $n = 2$ and $m = 1$ for the diurnal cases and $m = 2$ for the semi-diurnal cases. According to [4] the expression for U^{a}_{2} for a diurnal wave at frequency σ with $(n + m)$: *odd* is:

$$U^{a}_{n=2} = \overline{A}^{\sigma}_{21} \overline{P}_{21}(\cos\theta) \sin(\sigma(t) + m\lambda) \tag{8.19}$$

while the expression for U^{a}_{2} for a semi-diurnal wave at frequency σ with $(n + m)$: *even* is:

$$U^{a}_{n=2} = \overline{A}^{\sigma}_{22} \overline{P}_{22}(\cos\theta) \cos(\sigma(t) + m\lambda) \tag{8.20}$$

Time derivative of the elevation field

The $\partial_t \eta$ term in the $< \widehat{W_1} >$ integral is defined on basis of the choice of σ where we will only use the prograde component:

$$\frac{\partial \eta}{\partial t} = -\sigma \sum_{nma} D^+_{nm} \sin(\sigma(t) + m\lambda - \psi^+_{nm}) \overline{P}_{nm}(\cos\theta) \tag{8.21}$$

Phase definitions of the ocean and the astronomical tide generating potential are both controlled by the expression $\sigma(t)$ and the geographic longitude λ. Due to the fact that we average over a full tidal cycle T it doesn't really matter in which way $\sigma(t)$ is defined as long as it is internally consistent between $\partial_t \eta$ and Γ.

Result

We continue with the evaluation of $m = 1$ for diurnal waves and $m = 2$ for semi-diurnal waves and get:

$$< \widehat{D} > \; = \; \int_\Omega < \rho \Gamma \frac{\partial \eta}{\partial t} > \, d\Omega \; = \; W_{nm\sigma} D^+_{2m} \begin{bmatrix} -\cos\psi^+_{2m} \\ +\sin\psi^+_{2m} \end{bmatrix} \tag{8.22}$$

with $W_{nm\sigma} = 4\pi R^2 \rho (1 + k_2 - h_2) \sigma \overline{A}^\sigma_{2m}$ where R is the mean Earth radius and whereby $-\cos\psi^+_{2m}$ is evaluated for the diurnal tides and the $\sin\psi^+_{2m}$ for the semi diurnal tides. We remind that eq. (8.22) matches eq.(4.3.16) in [16]. The diurnal equivalent does however not appear in this reference and phase corrections of $\pm\pi/2$ should be applied. In addition we notice that we did not take into account the effect of self attraction and loading tides in the evaluation of the global dissipation rates although this effect is probably smaller than the oceanic effect. The closed expression for the self attraction and loading effect is:

$$< \widehat{D} > \; = \; W_{nm\sigma} D^+_{2m} \frac{3(1 + k'_2 - h'_2)\rho_w}{5\rho_e} \begin{bmatrix} -\cos\psi^+_{2m} \\ \sin\psi^+_{2m} \end{bmatrix} \tag{8.23}$$

which follows the same evaluation rules as eq.(8.22).

8.3 Global dissipation rates

We computed the global dissipation rates for eight tidal constituents which are considered to be energetic, meaning that their harmonic coefficients stand out in the tide generating potential. The rates corresponding to eqn. (8.22) for the diurnal constituents Q_1, O_1, P_1 and K_1 and the semi-diurnal constituents N_2 M_2 S_2 and K_2 are shown in table 8.1. For ρ we have used 1026 kg/m^3, $h_2 = 0.606$, $k_2 = 0.313$ and $R = 6378.137$ km.

The models in table 8.1 are selected on basis of several criteria. The main criteria are availability of the model, its ability to provide a global coverage of the oceans, documentation on the method to retrieve the in-phase and quadrature coefficient maps from the data.

	Q_1	O_1	P_1	K_1	N_2	M_2	S_2	K_2
SW80	0.007	0.176	0.033	0.297	0.094	1.896	0.308	0.024
FES94.1	0.007	0.174	0.035	0.321	0.097	2.324	0.350	0.027
FES95.2	0.007	0.186	0.035	0.310	0.111	2.385	0.390	0.027
FES99	0.008	0.185	0.033	0.299	0.109	2.438	0.367	0.028
SR950308	0.006	0.150	0.028	0.233	0.112	2.437	0.434	0.027
SR950308c	0.007	0.180	0.034	0.288	0.114	2.473	0.435	0.027
GOT99.2	0.008	0.181	0.032	0.286	0.110	2.414	0.428	0.029
TPXO5.1	0.008	0.186	0.032	0.293	0.110	2.409	0.376	0.030
NAO99b	0.007	0.185	0.032	0.294	0.109	2.435	0.414	0.035
CSR40	0.008	0.181	0.031	0.286	0.111	2.425	0.383	0.028
Mean	0.007	0.179	0.032	0.290	0.109	2.416	0.397	0.029
Sigma	0.001	0.012	0.002	0.024	0.005	0.042	0.031	0.002

Table 8.1: Dissipation rates of 10 tide models, the model labels are explained in the text, the average and standard deviations are computed over all models except SW80, units: Terrawatts

8.3.1 Models

The SW80 and the FES94.1 models did not rely on altimeter data and may be seen as purely hydrodynamic estimates of the ocean tides. The SW80 model is described in [9], [10] and [11] and is often referred to as the Schwiderski model providing at its time the first realistic hydrodynamic estimate of the ocean tides obtained by solving the Laplace tidal equations. An more modern version is the FES94.1 model. It is a finite element solution (FES) with the ability to follow the details of the tides in shallow waters. Version 94.1 is documented in the JGR Oceans special volume on the Topex/Poseidon altimetry system, see [17]. The FES95.2 model is a refinement of the FES94.1 model that relies on the representer technique described by [13] to assimilate TOPEX/Poseidon altimetry data. The FES99 model is new version of the FES95.2 model that incorporates a larger time span of the T/P data which comes in the form of spatially filtered altimetry data at a number of crossover locations. The FES99 model assimilates both T/P crossover data and tide gauge data.

In table 8.1 there are four empirical tide models that heavily rely on tidal constants directly estimated from the T/P altimeter data set. The SR950308 model is an updated version of the method documented by [7] and is based upon a local harmonic improvement of the in-phase and quadrature components relative to a background ocean tide model. Thereby it relies on the availability of T/P data an not so much on model dynamics. In the above table the SR950308 model is evaluated within latitude bands that follow from the orbit inclination of T/P. The SR950308c model is an identical version that is complemented by SW80 tidal constants outside the range of the SR950308 model. Both the SR models are based upon cycles 2 to 71 of T/P altimetry. Another empirical model is the GOT99.2 model that is documented in [23]. It is based on the same technique as described in [7] and can be seen as an update to the earlier approach in the sense that 232 TOPEX cycles are used rather than the 70 cycles available at the time the SR950308

model was developed.

The CSR4.0 model falls essentially in the same category of methods as the SR950308 and the GOT99.2 model. In essence it is an empirical estimation technique and an update to the CSR3.0 model documented in cf. [20]. The CSR4.0 model is based upon an implementation of a spectral response method that involves the computation of orthotides as described in the paper of [15]. Spectral response models enable to incorporate the effects of minor tidal lines in the calculation without separately estimating the individual harmonic coefficients of those lines. Without doubt this procedure relaxes the parameter estimation effort. A drawback of the used orthotide method is that resonance effects or energy concentrated at tidal cusps in the tides leak to neighboring lines.

Two other models that we included in table 8.1 are TPXO5.1 and NAO99b. The TPXO5.1 model is based upon the representer approach as described in [12] whereby TOPEX/POSEIDON crossover data is assimilated in the solution. It differs from the FES95.2 and FES99 models; the method of discretization and dynamical modelling are set-up in different ways. The NAO99b model, cf. [26], is also based upon a data assimilation technique. In this case a nudging technique rather than a representer technique is used.

8.3.2 Interpretation

Table 8.1 shows that most dissipation rates of the selected tide models differ by about 2%. The average global dissipation rate of M_2 is now 2.42 TW and its standard deviation is 0.04 TW. The SW80 and the FES94.1 models are the only two exceptions that underestimate the M_2 dissipation by respectively 0.5 and 0.1 TW. In [4] it is mentioned that this behavior is typical for most hydrodynamic models which depend for their dissipation rates on the prescribed drag laws in the model. All other post T/P models handle this problem in a different way, and are based upon assimilation techniques.

Other tidal constituents that stand out in the dissipation computations are O_1 K_1 and S_2. For the latter term it should be remarked that energy is not only dissipated in the ocean, but also in the atmosphere. This can be confirmed by comparing the S_2 dissipation to an independent geodetic estimate from satellite geodesy.

8.4 Exercises

- Why does orbital analysis of Lageos and Starlette give us a different value for the dissipation on S_2 compared to dissipation estimates from altimetry
- Is there an age limit on our solar system given the current rate tidal energy dissipation?
- How would you measure the rate of energy dissipation for M_2 in the North sea if transport measurements are provided at the boundary of a model for the North sea, and if tidal constants for η are provided within the numerical box?

Appendix A

Legendre Functions

Legendre functions appear when we solve the Laplace equation ($\nabla U = 0$) by means of the method of separation of variables. Normally the Laplace equation is transformed in spherical coordinates r, λ, θ (r: radius, λ: longitude θ: co-latitude); this problem can be found in section 10.8 in [3] where the well known solution for this problem is shown:

$$U(r, \lambda, \theta) = R(r)G(\lambda, \theta) \tag{A.1}$$

with:

$$R(r) = c_1 r^n + c_2 \frac{1}{r^{n+1}} \tag{A.2}$$

and where c_1 and c_2 are integration constants. Solutions of $G(\lambda, \theta)$ appear in a further separation of variables, these solutions are called surface harmonics and in [3] you will find that:

$$G(\lambda, \theta) = [A_{nm} \cos(m\lambda) + B_{nm} \cos(m\lambda)] \, P_{nm}(\cos\theta) \tag{A.3}$$

where also A_{nm} and B_{nm} are integration constants. The $P_{nm}(\cos\theta)$ functions are called associated Legendre functions and the indices n and m are called degree and order. When $m = 0$ we deal with zonal Legendre functions and for $m = n$ we are dealing with sectorial Legendre functions, all others are tesseral Legendre functions. The following table contains zonal Legendre functions up to degree 5 whereby $P_n(\cos\theta) = P_{n0}(\cos\theta)$:

$$\begin{aligned}
P_0(\cos\theta) &= 1 \\
P_1(\cos\theta) &= \cos\theta \\
P_2(\cos\theta) &= \frac{3\cos 2\theta + 1}{4} \\
P_3(\cos\theta) &= \frac{5\cos 3\theta + 3\cos\theta}{8} \\
P_4(\cos\theta) &= \frac{35\cos 4\theta + 20\cos 2\theta + 9}{64} \\
P_5(\cos\theta) &= \frac{63\cos 5\theta + 35\cos 3\theta + 30\cos\theta}{128}
\end{aligned}$$

Associated Legendre functions are obtained by differentiation of the zonal Legendre function, in particular:

$$P_{nm}(t) = (1 - t^2)^{m/2} \frac{d^m P_n(t)}{dt^m} \tag{A.4}$$

so that you obtain:

$$\begin{aligned}
P_{11}(\cos\theta) &= \sin\theta \\
P_{21}(\cos\theta) &= 3\sin\theta\cos\theta \\
P_{22}(\cos\theta) &= 3\sin^2\theta \\
P_{31}(\cos\theta) &= \sin\theta\left(\frac{15}{2}\cos^2\theta - \frac{3}{2}\right) \\
P_{32}(\cos\theta) &= 15\sin^2\theta\cos\theta \\
P_{32}(\cos\theta) &= 15\sin^3\theta
\end{aligned}$$

Legendre functions are orthogonal base functions in an L^2 function space whereby the inner product is defined as:

$$\int_{-1}^{1} P_{n'}(x)P_n(x)\,dx = 0 \qquad n' \neq n \tag{A.5}$$

and

$$\int_{-1}^{1} P_{n'}(x)P_n(x)\,dx = \frac{2}{2n+1} \qquad n' = n \tag{A.6}$$

In fact, these integrals are definitions of an inner product of a function space whereby $P_n(\cos\theta)$ are the base functions. Due to orthogonality we can easily develop an arbitrary function $f(x)$ for $x \in [-1, 1]$ into a so-called Legendre function series:

$$f(x) = \sum_{n=0}^{\infty} f_n P_n(x) \tag{A.7}$$

The question is to obtain the coefficients f_n when $f(x)$ is provided in the interval $x \in [-1, 1]$. To demonstrate this procedure we integrate on the right and left hand side of eq. $A.7$ as follows:

$$\int_{-1}^{1} f(x)P_{n'}(x)\,dx = \int_{-1}^{1} \sum_{n=0}^{\infty} f_n P_n(x)P_{n'}(x)\,dx \tag{A.8}$$

Due to the orthogonality relation of Legendre functions this right hand side integral reduces to an answer that only exists for $n = n'$:

$$\int_{-1}^{1} f(x)P_n(x)\,dx = \frac{2}{2n+1} f_n \tag{A.9}$$

so that:

$$f_n = \frac{2n+1}{2}\int_{-1}^{1} f(x)P_n(x)\,dx \tag{A.10}$$

This formalism may be expanded in two dimensions where we now introduce spherical harmonic functions:

$$Y_{nma}(\theta, \lambda) = \left\{ \begin{array}{c} \cos m\lambda \\ \sin m\lambda \end{array} \right\}_{a=0}^{a=1} P_{nm}(\cos\theta) \tag{A.11}$$

which are related to the associated Legendre functions. In turn spherical harmonic functions possess orthogonal relations which become visible when we integrate on the sphere, that is:

$$\int\int_{\sigma} Y_{nma}(\theta,\lambda)Y_{n'm'a'}(\theta,\lambda)\,d\sigma = \frac{4\pi(n+m)!}{(2n+1)(2-\delta_{0m})(n-m)!} \tag{A.12}$$

but only when $n = n'$ and $m = m'$ and $a = a'$.

Spherical harmonic functions $Y_{nma}(\theta,\lambda)$ are again basis functions of a function space whereby integral A.12 defines the inner product of the function space. We remark that spherical harmonic functions form an orthogonal set of basis functions since the answer of integral A.12 depends on degree n and the order m.

In a similar fashion spherical harmonic functions allow to develop an arbitrary function over the sphere in a spherical harmonic function series. Let this arbirary function be called $f(\theta,\lambda)$ and set as goal to find the coefficients C_{nma} in the series:

$$f(\theta,\lambda) = \sum_{n=0}^{\infty}\sum_{m=0}^{n}\sum_{a=0}^{1} C_{nma}Y_{nma}(\theta,\lambda) \tag{A.13}$$

This problem can be treated in the same way as for the zonal Legendre function problem, in fact, it is a general approach that may be taken for the subset of functions that can be developed in a series of orthogonal (or orthonomal) base functions. Thus:

$$\int\int_{\sigma} Y_{n'm'a'}(\theta,\lambda)f(\theta,\lambda)\,d\sigma = \int\int_{\sigma} Y_{n'm'a'}(\theta,\lambda)\sum_{n=0}^{\infty}\sum_{m=0}^{n}\sum_{a=0}^{1} C_{nma}Y_{nma}(\theta,\lambda)\,d\sigma \tag{A.14}$$

which is only relevant when $n = n'$ and $m = m'$ and $a = a'$. So that:

$$C_{nma} = N_{nm}^{-1}\int\int_{\sigma} Y_{nma}(\theta,\lambda)f(\theta,\lambda)\,d\sigma \tag{A.15}$$

where

$$N_{nm} = \frac{4\pi(n+m)!}{(2n+1)(2-\delta_{0m})(n-m)!} \tag{A.16}$$

A.1 Normalization

Normalization of Legendre functions is a separate issue that follows from the fact that we are dealing with an orthogonal set of functions. There are several ways to normalize Legendre functions, one choice is to rewrite integral Eq. A.12 into a *normalized* integral:

$$\frac{1}{4\pi}\int\int_{\sigma} \overline{Y}_{nma}(\theta,\lambda)\overline{Y}_{n'm'a'}(\theta,\lambda)\,d\sigma = 1 \tag{A.17}$$

where we simply defined new *normalized* functions with an overbar which are now called the normalized spherical harmonic functions. It is obvious that they rely on normalized associated Legendre functions:

$$\overline{P}_{nm}(\cos\theta) = \left[(2n+1)(2-\delta_{0m})\frac{(n-m)!}{(n+m)!}\right]^{1/2} P_{nm}(\cos\theta) \tag{A.18}$$

The use of normalized associated Legendre functions results now in an orthonormal set of spherical harmonic base functions as can be seen from the new definition of the inner product in eq. A.17. It is customary to use the normalized functions because of various reasons, a very important numerical reason is that stable recursive schemes for normalized associated Legendre functions exist whereas this is not necessarily the case for the unnormalized Legendre functions. This problem is beyond the scope of these lecture notes, the reader must assume that there is software to compute normalized associated Legendre functions up to high degree and order.

A.2 Some convenient properties of Legendre functions

A.2.1 Property 1

A well-known property that we often use in potential theory is the development of the function $1/r$ in a series of zonal Legendre functions. We need to be a bit more specific on this problem. Assume that there are two vectors $\overline{p}$ and $\overline{q}$ and that their length is r_p and r_q respectively. If the length of the vector $\overline{p} - \overline{q}$ is called r_{pq} then:

$$r_{pq} = \left(r_p^2 + r_q^2 - 2r_p r_q \cos\psi\right)^{1/2} \tag{A.19}$$

for which it is known that:

$$\frac{1}{r_{pq}} = \frac{1}{r_q} \sum_{n=0}^{\infty} \left(\frac{r_p}{r_q}\right)^n P_n(\cos\psi) \tag{A.20}$$

where ψ is the angle between $\overline{p}$ and $\overline{q}$. This series is convergent when $r_p < r_q$. The proof for this property is given in [21] and starts with a Taylor expansion of the test function:

$$r_{pq} = r_p \left(1 - 2su + s^2\right)^{1/2} \tag{A.21}$$

where $s = r_q/r_p$ and $u = \cos\psi$. The binomial theorem, valid for $|z| < 1$ dictates that:

$$(1-z)^{-1/2} = \alpha_0 + \alpha_1 z + \alpha_2 z^2 + ... \tag{A.22}$$

where $\alpha_0 = 1$ and $\alpha_n = (1.3.5...(2n-1))/(2.4...(2n))$. Hence if $|2su - s^2| < 1$ then:

$$(1 - 2su + s^2)^{-1/2} = \alpha_0 + \alpha_1(2su - s^2) + \alpha_2(2su - s^2)^2 + ... \tag{A.23}$$

so that:

$$\begin{aligned} (1 - 2su + s^2)^{-1/2} &= 1 + us + \frac{3}{2}(u^2 - \frac{1}{3})s^2 + ... \\ &= P_0(u) + sP_1(u) + s^2P_2(u) + ... \end{aligned}$$

which completes the proof.

A.2.2 Property 2

The addition theorem for Legendre functions is:

$$P_n(\cos\psi) = \frac{1}{2n+1}\sum_{ma}\overline{Y}_{nma}(\theta_p,\lambda_p)\overline{Y}_{nma}(\theta_q,\lambda_q) \tag{A.24}$$

where λ_p and θ_p are the spherical coordinates of vector $\overline{p}$ and λ_q and θ_q the spherical coordinates of vector $\overline{q}$.

A.2.3 Property 3

The following recursive relations exist for zonal and associated Legendre functions:

$$P_n(t) = -\frac{n-1}{n}P_{n-2}(t) + \frac{2n-1}{n}tP_{n-1}(t) \tag{A.25}$$

$$P_{nn}(\cos\theta) = (2n-1)\sin\theta P_{n-1,n-1}(\cos\theta) \tag{A.26}$$

$$P_{n,n-1}(\cos\theta) = (2n-1)\cos\theta P_{n-1,n-1}(\cos\theta) \tag{A.27}$$

$$P_{nm}(\cos\theta) = \frac{(2n-1)}{n-m}\cos\theta P_{n-1,m}(\cos\theta) - \frac{(n+m-1)}{n-m}P_{n-2,m}(\cos\theta) \tag{A.28}$$

$$P_{n,m}(\cos\theta) = 0 \quad \text{for } m > n \tag{A.29}$$

For differentiation the following recursive relations exist:

$$(t^2-1)\frac{dP_n(t)}{dt} = n\left(tP_n(t) - P_{n-1}(t)\right) \tag{A.30}$$

A.3 Convolution integrals on the sphere

Spherical harmonic function expansions are very convenient for the evaluation of the following type of convolution integrals on the sphere:

$$H(\theta,\lambda) = \int_\Omega F(\theta',\lambda')G(\psi)\; d\Omega \tag{A.31}$$

where $d\Omega = \sin\psi\, d\psi\, d\alpha$ and ψ the spherical distance between θ,λ and θ',λ' and α the azimuth. In eq. $(A.31)$ the F and G function are written as:

$$F(\theta,\lambda) = \sum_{n=0}^{\infty}\sum_{m=0}^{n}\sum_{a=0}^{1}F_{nma}\overline{Y}_{nma}(\theta,\lambda) \tag{A.32}$$

where

$$\begin{aligned}\overline{Y}_{nm,0}(\theta,\lambda) &= \cos(m\lambda)\overline{P}_{nm}(\cos\theta)\\ \overline{Y}_{nm,1}(\theta,\lambda) &= \sin(m\lambda)\overline{P}_{nm}(\cos\theta)\end{aligned}$$

and

$$G(\psi) = \sum_{n=0}^{\infty}G_nP_n(\cos\psi) \tag{A.33}$$

It turns out that instead of numerically computing the expensive surface integral in eq. (A.31) that it is easier to multiply the G_n and F_{nma} coefficients:

$$H(\theta,\lambda) = \sum_{n=0}^{\infty}\sum_{m=0}^{n}\sum_{a=0}^{1} H_{nma}\overline{Y}_{nma}(\theta,\lambda) \tag{A.34}$$

where

$$H_{nma} = \frac{4\pi G_n}{2n+1}F_{nma} \tag{A.35}$$

A.3.1 Proof

For completeness we also present the proof of eq. (A.35): The addition theorem of Legendre functions states that:

$$P_n(\cos\psi_{pq}) = \frac{1}{2n+1}\sum_{m=0}^{n}\overline{P}_{nm}(\cos\theta_p)\overline{P}_{nm}(\cos\theta_q)\cos(m(\lambda_p-\lambda_q)) \tag{A.36}$$

which is equal to

$$P_n(\cos\psi_{pq}) = \frac{1}{2n+1}\sum_{m=0}^{n}\sum_{a=0}^{1}\overline{Y}_{nm}(\theta_p,\lambda_p)\overline{Y}_{nm}(\theta_q,\lambda_q) \tag{A.37}$$

If this property is substituted in eq. (A.31) then:

$$H(\theta,\lambda) = \int_\Omega \left\{\sum_{nma} F_{nma}\overline{Y}_{nma}(\theta',\lambda')\right\}\left\{\sum_{n'm'a'}\frac{G_{n'}}{2n'+1}\overline{Y}_{n'm'a'}(\theta,\lambda)\overline{Y}_{n'm'a'}(\theta',\lambda')\right\} d\Omega \tag{A.38}$$

which is equal to:

$$H(\theta,\lambda) = \sum_{n'm'a'}\frac{G_{n'}}{2n'+1}\overline{Y}_{n'm'a'}(\theta,\lambda)\sum_{nma}F_{nma}\int_\Omega \overline{Y}_{nma}(\theta',\lambda')\overline{Y}_{n'm'a'}(\theta',\lambda')\,d\Omega \tag{A.39}$$

Due to orthogonality properties of normalized associated Legendre functions we get the desired relation:

$$H(\theta,\lambda) = \sum_{nma}\frac{4\pi G_n}{2n+1}F_{nma}\overline{Y}_{nma}(\theta,\lambda) \tag{A.40}$$

which completes our proof.

Appendix B

Tidal harmonics

Section 2.3.1 introduced the concept of tidal harmonics. Purpose of this section is to present the implementation of a method to obtain the tables and to present the results. The method used here to compute tidal harmonics in Cartwright Tayler and Edden differs from the approach used in this lecture notes. In contrast to CTE, who used several convolution operators to separate tidal groups. Here we rely on an algorithm that assumes a least squares fitting procedure and prior knowledge of all Doodson numbers in the summation over all frequencies indicated by index v. To obtain the tidal harmonic coefficients $H^{(v)}$ for each Doodson number the following procedure is used:

- For each degree n and tidal species m (which equals k_1) the algorithm starts to collect all matching Doodson numbers.
- The following step is to generate values of:

$$U^a_{nm}(t) = \frac{\mu_b (r_e / r_{eb}(t))^n}{(2n+1) r_{eb}(t)} \times P_{nm}(\cos\theta_b(t)) \times \cos(m\lambda_b(t))$$

  where t is running between 1990/1/1 00:00 and 2010/1/1 00:00 in a sufficiently dense number of steps to avoid under sampling. Positions of Sun and Moon obtained from a planetary ephemeris model are used to compute the distance $R_{eb}(t)$ between the astronomical body (indicated by subscript b) and the Earth's center (indicated by subscript e) are transformed into Earth-fixed coordinates to obtain $\theta_b(t)$ and $\lambda_b(t)$.

- The following step is a least squares analysis of $U_{nm}(t)$ where the observations equations are as follows:

$$U^a_{nm}(t) = \sum_{v'} G^{(v')} \cos(X_{v'})$$

  when $m+n$ is even and

$$U^a_{nm}(t) = \sum_{v'} G^{(v')} \sin(X_{v'})$$

  whenever $m+n$ is odd. The v' symbol is used to indicate that we are only considering the appropriate subset of Doodson numbers to generate the $X_{v'}$ values, see also section 2.3.1.

- Finally the $G^{v'}$ values need a scaling factor to convert them into numbers that have the same dimension as one finds in CTE. Partly this conversion is caused by a different normalization between surface harmonics used in CTE and eqns. (2.13), (2.14) and (2.15) here, although is it also required to take into account the factor g. As a result:

$$H^{v'} = G^{v'} g^{-1} f_{nm}^{-1} \Pi_{nm}^2$$

  where Π_{nm} is the normalization factor as used in appendix A and f_{nm} the normalization factor used by CTE given in eqns. (2.16) and (2.17). In our algorithm g is computed as μ/r_e^2 where $\mu = 3.9860044 \times 10^{14}$ $[m^3/s^2]$ and $r_e = 6378137.0$ $[m]$.

For all collected spectral lines we show in table B.1 and B.2 only those where $|H^{(v)}|$ exceeds the value of 0.0025. Tables B.1 and B.2 show in columns 2 to 7 the values of k_1 till k_6, in column 8 the degree n, in column 9 the coefficient H^v in equations (2.14) and (2.15), in column 10 the Darwin symbol provided that it exists, and in column 11 the Doodson number.

Some remarks about the tables: a) The tables only hold in the time period indicated earlier in this chapter, b) There are small differences, mostly in the 5th digit behind the period, with respect to the values given in [4], c) In total we have used 484 spectral lines although many more tidal lines may be observed with a cryogenic gravimeter.

	k_1	k_2	k_3	k_4	k_5	k_6	n	$H^{(v)}$	Darwin	Doodson
1	0	0	0	0	0	0	2	-.31459	$M_0 + S_0$	055.555
2	0	0	0	0	1	0	2	.02793		055.565
3	0	0	1	0	0	-1	2	-.00492	Sa	056.554
4	0	0	2	0	0	0	2	-.03099	Ssa	057.555
5	0	1	-2	1	0	0	2	-.00673		063.655
6	0	1	0	-1	-1	0	2	.00231		065.445
7	0	1	0	-1	0	0	2	-.03518	Mm	065.455
8	0	1	0	-1	1	0	2	.00228		065.465
9	0	2	-2	0	0	0	2	-.00584		073.555
10	0	2	0	-2	0	0	2	-.00288		075.355
11	0	2	0	0	0	0	2	-.06660	Mf	075.555
12	0	2	0	0	1	0	2	-.02761		075.565
13	0	2	0	0	2	0	2	-.00258		075.575
14	0	3	-2	1	0	0	2	-.00242		083.655
15	0	3	0	-1	0	0	2	-.01275		085.455
16	0	3	0	-1	1	0	2	-.00529		085.465
17	0	4	-2	0	0	0	2	-.00204		093.555
18	1	-3	0	2	0	0	2	.00664		125.755
19	1	-3	2	0	0	0	2	.00801	σ_1	127.555
20	1	-2	0	1	-1	0	2	.00947		135.645
21	1	-2	0	1	0	0	2	.05019	Q_1	135.655
22	1	-2	2	-1	0	0	2	.00953	ρ_1	137.455
23	1	-1	0	0	-1	0	2	.04946		145.545
24	1	-1	0	0	0	0	2	.26216	O_1	145.555
25	1	-1	2	0	0	0	2	-.00343		147.555
26	1	0	0	-1	0	0	2	-.00741		155.455
27	1	0	0	1	0	0	2	-.02062	M_1	155.655
28	1	0	0	1	1	0	2	-.00414		155.665
29	1	0	2	-1	0	0	2	-.00394		157.455
30	1	1	-3	0	0	1	2	.00713	π_1	162.556
31	1	1	-2	0	0	0	2	.12199	P_1	163.555
32	1	1	-1	0	0	1	2	-.00288	S_1	164.556
33	1	1	0	0	-1	0	2	.00730		165.545
34	1	1	0	0	0	0	2	-.36872	K_1	165.555

Table B.1: Tidal harmonic constants

	k_1	k_2	k_3	k_4	k_5	k_6	n	$H^{(v)}$	Darwin	Doodson
35	1	1	0	0	1	0	2	-.05002		165.565
36	1	1	1	0	0	-1	2	-.00292	ψ_1	166.554
37	1	1	2	0	0	0	2	-.00525	ϕ_1	167.555
38	1	2	-2	1	0	0	2	-.00394	τ_1	173.655
39	1	2	0	-1	0	0	2	-.02062	J_1	175.455
40	1	2	0	-1	1	0	2	-.00409		175.465
41	1	3	-2	0	0	0	2	-.00342		183.555
42	1	3	0	0	0	0	2	-.01128	OO_1	185.555
43	1	3	0	0	1	0	2	-.00723		185.565
44	1	4	0	-1	0	0	2	-.00216		195.455
45	2	-3	2	1	0	0	2	.00467		227.655
46	2	-2	0	2	0	0	2	.01601	$2N_2$	235.755
47	2	-2	2	0	0	0	2	.01932	μ_2	237.555
48	2	-1	0	1	-1	0	2	-.00451		245.645
49	2	-1	0	1	0	0	2	.12099	N_2	245.655
50	2	-1	2	-1	0	0	2	.02298	ν_2	247.455
51	2	0	-1	0	0	1	2	-.00217		254.556
52	2	0	0	0	-1	0	2	-.02358		255.545
53	2	0	0	0	0	0	2	.63194	M_2	255.555
54	2	1	-2	1	0	0	2	-.00466		263.655
55	2	1	0	-1	0	0	2	-.01786	L_2	265.455
56	2	1	0	1	0	0	2	.00447		265.655
57	2	2	-3	0	0	1	2	.01719	T_2	272.556
58	2	2	-2	0	0	0	2	.29401	S_2	273.555
59	2	2	-1	0	0	-1	2	-.00246		274.554
60	2	2	0	0	0	0	2	.07992	K_2	275.555
61	2	2	0	0	1	0	2	.02382		275.565
62	2	2	0	0	2	0	2	.00259		275.575
63	2	3	0	-1	0	0	2	.00447		285.455
64	0	1	0	0	0	0	3	-.00375		065.555
65	1	0	0	0	0	0	3	.00399		155.555
66	2	-1	0	0	0	0	3	-.00389		245.555
67	2	1	0	0	0	0	3	.00359		265.555
68	3	-1	0	1	0	0	3	-.00210		345.655
69	3	0	0	0	0	0	3	-.00765		355.555

Table B.2: Tidal harmonic constants

Bibliography

[1] Gill A.E. *Atmosphere-Ocean Dynamics*. Academic Press, 1982.

[2] Le Provost C. and F. Lyard. Energetics of the M_2 barotropic ocean tides: an estimate of bottom friction dissipation from a hydrodynamic model. *Progress in Oceanography*, 40:37–52, 1997.

[3] Wylie C.R. and L.C. Barrett. *Advanced Engineering Mathematics*. McGraw-Hill, 1982.

[4] Cartwright D.E. *Theory of Ocean Tides with Application to Altimetry*, volume 50. Springer Verlag, Lecture notes in Earth Sciences, R. Rummel and F. Sansò (eds), 1993.

[5] Cartwright D.E. *Tides, A Scientific History*. Cambridge University Press, 1999.

[6] Cartwright D.E. and W. Munk. Tidal spectroscopy and prediction. *Philosophical Transactions of the Royal Society*, A259:533–581, 1966.

[7] Schrama E.J.O. and R.D. Ray. A preliminary tidal analysis of TOPEX/POSEIDON altimetry. *Journal of Geophysical Research*, C99:24799–24808, 1994.

[8] Dickey J.O. et al. Lunar Laser Ranging, A Continuing Legacy of the Apollo Program. *Science*, 265:482–490, 1994.

[9] Schwiderski E.W. Ocean tides, I, global tidal equations. *Marine Geodesy*, 3:161–217, 1980.

[10] Schwiderski E.W. Ocean tides, II, a hydrodynamic interpolation model. *Marine Geodesy*, 3:219–255, 1980.

[11] Schwiderski E.W. Atlas of ocean tidal charts and maps, I, the semidiurnal principal lunar tide M_2. *Marine Geodesy*, 6:219–265, 1983.

[12] Egbert G.D. Tidal data inversion: interpolation and inference. *Progress in oceanography*, 40:53–80, 1997.

[13] Egbert G.D. and Bennett A.F. Data assimilation methods for ocean tides. *Elsevier Press, Modern Approaches to Data Assimilation in Ocean Modelling, P. Malanotte-Rizzoli (eds)*, 1996.

[14] Egbert G.D. and R.D. Ray. Significant dissipation of tidal energy in the deep ocean inferred from satellite altimeter data. *Nature*, 405:775–778, 2000.

[15] Groves G.W. and Reynolds R.W. An orthogonolized convolution method of tide prediction. *Journal of Geophysical Research*, 80:4131–4138, 1975.

[16] Lambeck K. *Geophysical Geodesy, The Slow Deformations of the Earth.* Oxford Science Publications, 1988.

[17] Le Provost C. Genco M.L. Lyard F. Vincent P. Canceil P. Tidal spectroscopy of the world ocean tides from a finite element hydrodynamical model. *Journal of Geophysical Research*, 99(C12):24777–24798, 1994.

[18] Melchior P. *The Tides of the Planet Earth.* Pergamon Press, 1981.

[19] Pedlosky. *Geophysical Fluid Dynamics.* Springer-Verlag, New York (2nd ed.), 1987.

[20] Eanes R. and S. Bettadpur. The csr3.0 global ocean tide model: diurnal and semi-diurnal ocean tides from topex/poseidon altimetry. Technical Report CSR-TM-96-05, University of Texas at Austin, Center of Space Research, 1996.

[21] Rummel R. *Lecture notes physical geodesy (s50).* TU Delft, Department of geodesy, 1983.

[22] B.J. Chao Ray R.D., R.J. Eanes. Detection of tidal dissipation in the solid earth by satellite tracking and altimetry. *Nature*, 381:595–597, 1996.

[23] Ray R.D. A Global Ocean Tide Model from TOPEX/POSEIDON Altimetry: GOT99.2. Technical Report NASA/TM – 1999 – 209478, NASA Goddard Space Flight Center, 1999.

[24] Pagiatakis S. The response of a realistic earth to ocean tide loading. *Geophysical Journal International*, 103:541–560, 1990.

[25] Pond S. and Pickard G.L. *Introductory Dynamical Oceanography 2nd edition.* Pergamon Press, 1983.

[26] Matsumoto K. Takanezawa T. and M. Ooe. Ocean tide models developed by assimilating topex/poseidon altimeter data into hydrodynamical model: A global model and a regional model around japan. *Journal of Oceanography*, 56:567–581, 2000.

[27] Farrell W.E. Deformation of the earth by surface loads. *Rev.Geoph. and Space Phys.*, 10:761–797, 1972.

[28] Munk W.H. Once again: once again – tidal friction. *Progress in Oceanography*, 40:7–35, 1997.

[29] Munk W.H. and G.J.F. MacDonald. *The Rotation of the Earth, a Geophysical Discussion.* Cambridge University Press, 1960.

[30] Munk W.H. and C. Wunsch. Abyssal recipes II: Energetics of tidal and wind mixing. *Deep-Sea research*, 45:1977–2010, 1998.